UNIVERSITY OF
KWAZULU-NATAL

INYUVESI
YAKWAZULU-NATALI

Involvement of MAPK and Akt in the immunotoxicity of Fusaric Acid on Healthy Peripheral Blood Mononuclear Cells (PBMC) and Acute Monocytic Leukemic (Thp-1) Cells

By

SHANEL DHANI

BSc. B. Med Sc. (Hons) (UKZN)

Submitted in fulfillment of the requirements for the degree of

Master of Medical Science

In the

Discipline of Medical Biochemistry and Chemical Pathology

School of Laboratory of Medicine and Medical Science

College of Health Sciences

University of KwaZulu-Natal

Durban

2015

DECLARATION

This study represents the original work by the author and has not been submitted in any form to another university. The use of work by others has been duly acknowledged in the text.

The research described in this study was carried out in the Discipline of Medical Biochemistry, Faculty of Health Sciences, University of KwaZulu-Natal, Durban, under the supervision of Professor A.A Chuturgoon, Miss S Nagiah and Miss D.B Naidoo

Shanel Dhani

ACKNOWLEDGEMENTS

GOD

Through your grace and love I have come thus far and I thank you for everything in my life.

Professor A.A Chuturgoon

Your encouragement and advise has taught me that the greatest weapon to fight the world with is education. I am extremely grateful to you for motivating me and being an inspiration. Today I believe in myself and thus want to go further and achieve my goals. Thank you for sacrificing time off your busy schedule whenever I needed your assistance. Your trust and belief in me has inspired me and I feel honored to be associated with you. My achievement will not only benefit myself but also improve the lives of my parents and siblings, and I thank you a million times for giving us this hope, and pray for God's blessing to be upon you always.

Miss S Nagiah

My sincere gratitude goes to you for your unwavering support and guidance. You always went the extra mile in assisting me in spite of your heavy workload. I have learnt tremendously from you because you shared your knowledge unselfishly. All your effort and sacrifices is highly appreciated. I wish you all the best in your future endeavors, and may God grant you the wisdom in fulfilling your dreams.

Miss D.B Naidoo

My heartfelt appreciation for your kind assistance and perseverance throughout my work. When things were not turning out as I desired you stood by my side. You made me build up my confidence and take on those challenges. You have been a superb mentor. Thank you for your honesty and loving, caring support. May all your dream and aspirations come true.

Study participants

Thank you for donating blood samples effortlessly and being so efficient. As a result, I could continue my work timeously.

My parents

Thank you for laying the foundation for me at an early age in regards to my education. I appreciate all your love, support and sacrifices. I am eternally grateful to you. You are my pillar of strength. I am truly blessed having you as my parents.

PRESENTATIONS

S. Dhani, S. Nagiah, D.B Naidoo and A.A Chuturgoon

College of Health Science Research Symposium, University of KwaZulu-Natal, Durban, South Africa (September 2015)

TABLE OF CONTENTS

LIST OF FIGURES

CHAPTER 1

CHAPTER 2

CHAPTER 3

LIST OF TABLES

CHAPTER 3

LIST OF APPENDICES

LIST OF ABBREVIATIONS

α	Alpha
β	Beta
δ	Delta
γ	Gamma
µg	Microgram
µl	Microliter
µM	Micromolar
ºC	Degree Celsius
%	Percentage
4-HNE	4-Hydroxy 2-nonenal
ADP	Adenosine triphosphate
Akt	Protein kinase B
ANT	Adenine nucleotide transporter
ASK1	Apoptosis signal-regulating kinase 1
ATP	Adenosine Triphosphate
BCA	Bicinchoninic acid
Bcl-2	B-cell lymphoma 2
BSA	Bovine serum albumin
cm^3	Centimeter cube
CO_2	Carbon dioxide
Cu^+	Cuprous ion
Cu^{2+}	Copper ion
dH_2O	Distilled water
DISC	Death inducing signaling complex
DNA	Deoxyribonucleic acid
ELISA	Enzyme-linked immunosorbent assay
ER	Endoplasmic reticulum
ERK	Extracellular signal-regulated kinase
ETC	Electron transport chain
FA	Fusaric Acid
FAD	Flavin adenine dinucleotide dihydrogen
FADD	Fas-associated death domain
$FADH_2$	Flavin adenine dinucleotide
FCS	Foetal calf serum

FOXO	Forkhead
GTP	Guanosine triphosphate
h	Hour
HCl	Hydrogen Chloride
H_2O_2	Hydrogen peroxide
H_2SO_4	Sulphuric acid
H_3PO_4	Phosphoric acid
HRP	Horseradish peroxidase
hrs	Hours
IAP	Inhibitor of apoptosis protein
IC_{50}	half maximum inhibition
i.e.	that is
IGFIR	Insulin-like growth factor I receptor
JNK	c-Jun N-terminal kinase
kDa	Kilo Dalton
KCl	Potassium Chloride
M	Molar
mA	Milliampere
MAPK	Mitogen-activated protein kinase
MAPKK	Mitogen-activated protein kinase kinase
MAPKKK	Mitogen-activated protein kinase kinase kinase
MDA	Malondialdehyde
MEK	MAP/ERK kinase
mg	Milligram
min	Minute
MK	MAPK-activated protein kinase
ml	Milliliter
MLK	Mixed-lineage kinase
mM	Millimolar
MNK	MAPK-interacting kinase
mPTP	Mitochondrial permeability transition pore
mRNA	Messenger RNA
MSK	Mitogen-and-stress-activated kinase
NaCl	Sodium Chloride
NAD^+	Nicotinamide adenine diphosphate
NADPH	Nicotinamide adenine diphosphate phosphate hydrogen

NFDM	Non-fat dry milk
NK	Natural killer
nm	Nanometer
PA	Picolinic acid
PBMC	Peripheral blood mononuclear cells
PCD	Programmed cell death
PBS	Phosphate buffer saline
pg	Picogram
PH	Pleckstrin homology
PI	Propidium iodide
PI3K	Phosphatidylinositol 3-kinase
PIP3	Phosphatidylinositol 3,4,5- triphosphate
PMA	Phorbol 12-myristate 13-acetate
PUFA	Polyunsaturated fatty acids
RNS	Reactive nitrogen species
ROS	Reactive oxygen species
RLU	Relative light units
RT	Room temperature
SAPK	Stress activated protein kinase
SDS	Sodium dodecyl sulphate
SDS-PAGE	Sodium dodecyl sulphate -polyacrylamide gel electrophoresis
SOD	Superoxide dismutase
TAK1	Transforming growth factor β-activated kinase 1
TBARS	Thiobarbituric acid reactive substances
Th	T helper
Thp-1	Acute monocytic leukaemic cell
TNF-α	Tumour necrosis factor-α
TNFR1	Tumour necrosis factor receptor 1
TRADD	TNF-α receptor associated death domain
Treg	T regulatory
TTBS	Tris buffer saline with tween 20
UV	Ultraviolet
WST-1	Water soluble tetrazolium-1

ABSTRACT

Fusaric acid is a divalent chelator with moderate toxicity in plant and animals. However, studies lack on its effect on human models and the immune system. This study investigated the immunotoxicity of FA on PBMCs and Thp-1 cells. Cell viability was determined using the WST-1 assay and the mode of cell death by flow cytometry using the annexin V-FITC stain. Caspase 8, 9 and 3/7 activities were determined using Caspase-Glo assay®. TNF-α levels were measured using the TNF-α ELISA kit. Oxidative damage (MDA) was determined using the TBARS assay. Flow cytometry was performed to determine mitochondrial function using the JC-1 stain. ATP levels were measured using the ATP CellTitre Glo reagent. Western blotting was performed to determine protein expressions of Bax, p-Bcl-2, p-Akt, p-ERK, p-JNK and p38. The immunotoxicity of FA was confirmed by the decreased cell viability of PBMCs and Thp-1 cells and was validated by the externalization of phosphatidylserine on both PBMCs ($p<0.005$) and Thp-1 cells ($p<0.0001$). In PBMCs, FA induced paraptosis, evidenced by the decreased caspase 8 ($p<0.005$), 9 ($p<0.05$) and 3/7 ($p<0.005$) activities. Whilst in Thp-1 cells, FA induced intrinsic apoptosis supported by a decrease in caspase 8 activity ($p<0.05$) and an increase in caspase 9 ($p<0.05$) and 3/7 ($p<0.005$) activities; corresponding with unchanged TNF-α levels in both PBMCs ($p=0.3015$) and Thp-1 cells ($p=0.4540$). In PBMCs, FA significantly decreased Bax (pro-apoptotic) protein expression ($p<0.05$) and increased p-Bcl-2 (anti-apoptotic) protein expression ($p<0.05$) thereby maintaining mitochondrial membrane potential ($p=0.5643$). In Thp-1 cells, FA had no effect on the protein expression of Bax ($p=0.6130$) but significantly decreased the protein expression of p-Bcl-2 ($p<0.005$) with a corresponding increase in mitochondrial depolarization ($p<0.005$). In addition, FA increased oxidative stress (MDA levels) in both PBMCs ($p<0.005$) and Thp-1 cells ($p<0.005$) contributing to cellular damage and cellular signaling; and substantially decreased ATP levels in both PBMCs ($p<0.005$) and Thp-1 cells ($p<0.005$). Additionally, FA significantly increased phosphorylation of p-ERK (42kDa - $p<0.05$; 44kDa - $p<0.005$), p-JNK (46kDa - $p<0.005$; 54kDa - $p<0.05$) and p38 ($p<0.05$); and slightly increased the phosphorylation of p-Akt ($p=0.1640$) in PBMCs treated with FA. In Thp-1 cells, FA significantly up-regulated p-Akt ($p<0.05$) and p-ERK (42kDa - $p<0.0001$; 44kDa - $p<0.005$) expressions and significantly decreased p-JNK (46kDa - $p<0.05$; 54kDa - $p<0.005$) expression but had no effect on the expression of p38 ($p=0.8446$). This suggests the involvement of MAPK signaling in the induction of cell death in PBMCs and Thp-1 cells treated with FA. This study found that FA is immunotoxic to healthy human PBMCs and Thp-1 cells.

CHAPTER 1

1. INTRODUCTION

The mycotoxin, Fusaric Acid (FA), is a natural contaminant of maize and other cereal grains infected with *Fusarium* species (Bacon *et al.,* 1996). The toxicity of FA is due to its ability to chelate divalent ions important for cellular function (Amin *et al.,* 2001; Bochner *et al.,* 1980) and has being exemplified in various plant and animal species.

Numerous studies in plants documented the induction of apoptosis upon exposure to FA. Apoptotic cell death is commonly distinguished by molecular markers such as caspase activation and the externalisation of phosphatidylserine on plasma membranes in cells (Auffray *et al.,* 2009). Apoptosis transpires via the intrinsic or extrinsic apoptotic pathway (Auffray *et al.,* 2009). The intrinsic apoptotic pathway occurs via the mitochondria (Hemmati *et al*., 2002; Wan *et al.,* 2008). Bcl-2 stabilises the mitochondrial membrane potential by maintaining membrane integrity (Wan *et al.,* 2008; Adati *et al.,* 2009). Whilst, Bax antagonises the actions of Bcl-2 compromising the mitochondrial membrane integrity resulting in the release of cytochrome c and the subsequent activation of caspases and the induction of intrinsic apoptosis (Marchi *et al.,* 2011; Barrera, 2012; Morrison, 2012). The extrinsic apoptotic pathway is stimulated in response to binding of ligands (Morrison, 2012). Activation of the receptor results in the formation of a death domain that associates with the receptor (Eimon *et al*., 2006; Morrison, 2012). The death domain recruits initiator caspases forming a death inducing signalling complex (Elmore, 2007; Adati *et al*., 2009). The formation of this complex results in the activation of caspases and the induction of extrinsic apoptosis (Elmore, 2007; Adati *et al.,* 2009).

Intracellular stimuli such as reactive oxygen species (ROS) tend to regulate mitogen-activated protein kinase (MAPK) and protein kinase B (Akt) signalling (Kim *et al.,* 2014). The mitochondrial electron transport chain (ETC) is a major contributor in the production of ROS (Gutterman, 2005; Dayem *et al.,* 2010). The ETC synthesizes ATP and generates ROS as a by-product (Harper *et al.,* 2004). Under normal conditions, levels of ROS are maintained by antioxidant proteins; however, when these levels exceed the capacity of anti-oxidant proteins it results in oxidative stress (Harper *et al.,* 2004) and damage to macromolecules such as proteins, DNA and lipids (Son *et al*., 2011; Barrera, 2012).

The MAPK family comprises of three universal serine/threonine protein kinases; these include the extracellular signal-regulated kinase (ERK), c-Jun N-terminal kinase (JNK) and p38 kinase (Dhillon *et al*., 2007; Son *et al.,* 2011). Each group of MAPK is activated via a series of phosphorylation

events (Son *et al.*, 2011). The first event involves the phosphorylation and activation of a MAPK kinase kinase (MAPKKK), which in turn, phosphorylates and activates a MAPK kinase (MAPKK). MAPKKs activate MAPKs through dual phosphorylation on both threonine and tyrosine residues located within the tri-peptide motif of the MAPK (Boldt *et al*., 2002; Dhillon *et al*., 2007; Roux and Blenis, 2004; Cuenda and Rousseau, 2007). Once activated, MAPKs phosphorylate several transcription factors at serine and threonine residues, thereby regulating gene expression and cellular functions ranging from cell survival to cell death (Roux and Blenis, 2004; Morrison, 2012). Akt, another serine/threonine kinase, is a central mediator of cellular responses such as metabolism, cell survival and death, differentiation and mitosis (Wang *et al.*, 2015); and its signaling pathway is regularly activated simultaneously with ERK MAPK (Mertlikova-Kaiserova *et al.*, 2012; Mendoza *et al.*, 2011). Studies have shown that ROS act as second messengers in the activation of MAPK and Akt signaling pathways (Son *et al.*, 2011).

Preliminary research established the biological effect of FA in several plant and animal species. However, to date, no study has investigated the molecular toxicity of FA on human models, especially its effect on the immune system. Thus, this study aimed to assess the immunotoxicity of FA and the molecular events leading to the immunotoxicity in healthy human peripheral blood mononuclear cells (PBMCs) and Thp-1 cells. The objectives of the study were to determine the effect of FA on both PBMC and Thp-1 cell viability and the mode of cell death induced. Additionally, the study determined the effect of FA on specific cell death markers, oxidative stress, expression of apoptotic markers and the expression of MAPK and Akt kinases in both cell lines. It was hypothesized that FA is immunotoxic to PBMCs and Thp-1 cells via MAPK and Akt signalling.

2. LITERATURE REVIEW

2.1. Fusaric Acid (FA)

Endophytic fungi produce several secondary metabolites which behave as mycotoxins (Murphy *et al.*, 2006). Fusaric acid, also known as 5-butylpicolinic acid, is a picolinic acid (PA) derivative produced by several strains of Fusarium species such as *Fusarium moniliforme, F. heterosporum, F. oxysporum, F. solani,* and *F. proliferatum* (Amin *et al.*, 2001; Harper *et al.* 2004). Universally, these strains are known to parasitize maize and other cereal grains (Figure 1.1) (Wang and Ng, 1999).

Figure 1.1: Maize infected with *Fusarium Gibberella fujikuroi*. Pinkish-red discolouration is a characteristic of *Fusarium* infected tissue. **(Dragich and Nelson, 2014).**

2.1.1. Chemical structure of Fusaric Acid

The chemical structure of FA resembles its parent compound in that both contain a pyridine ring and a carboxylic acid substituent. The addition of the butyl group on the pyridine ring enables FA to permeate membranes much easier than PA (Figure 1.2A and 1.2B) (Kim *et al.*, 2014).

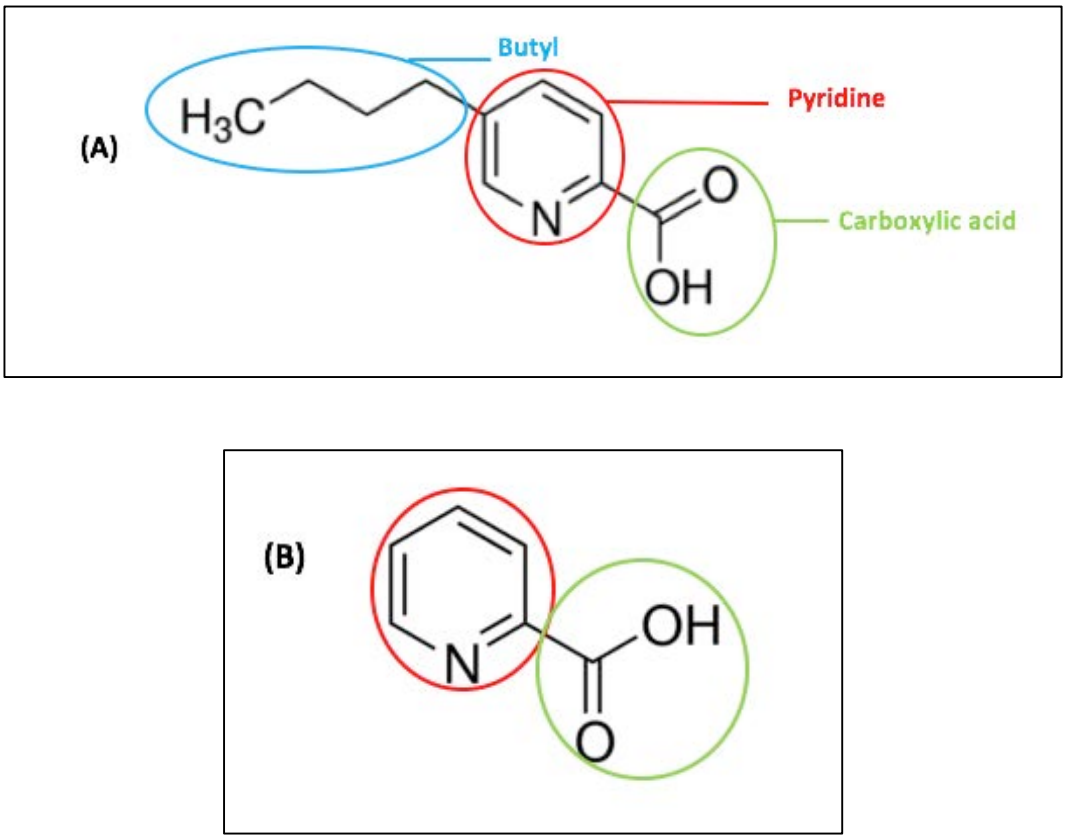

Figure 1.2: Chemical structure of Fusaric Acid (A) and Picolinic Acid (B). (Prepared by author).

2.1.2. Toxicity of Fusaric acid

The toxicity of FA is due to its ability to chelate divalent ions such as magnesium, calcium, zinc and iron (Amin *et al.*, 2001; Kuznetsov *et al.*, 2011). The nitrogen present in the pyridine ring and the deprotonated, negatively charged oxygen on the carboxylic acid group are responsible for FA's divalent chelating ability (Figure 1.2A) (Gutterman, 2005; Kwiatkowski *et al*., 1989).

2.1.3. Pharmacology of Fusaric Acid

2.1.3.1. In plants

Studies have shown that FA is phytotoxic to plants. Universally, FA causes wilt disease in numerous plants and has been reported to alter the permeability of membranes, increase electrolyte leakage, alter membrane potential and inhibit ATP synthesis (D'Alton and Etherton, 1984; Pavlovkin *et al.*, 2004). Many studies have reported toxic effects of FA, such as decreased cell viability and decreased ROS production, at concentrations greater than 10^{-5} M (Bharathiraja *et al.*, 2010). In support of this, another study done on the effect of FA on corn roots showed inhibition of the electron flux between

the succinate dehydrogenase and coenzyme Q, and inhibition of ATP synthase activity in the electron transport chain in isolated mitochondria (Diniz and Oliveira, 2009). In addition, FA caused lipid peroxidation in watermelon leaves and damaged the defense system in watermelon seedlings (Diniz and Oliveira, 2009).

2.1.3.2. In animals

In animals, FA inhibits the activity of the enzyme dopamine-β-hydroxylase and the synthesis of nucleic acids (Bharathiraja *et al*., 2010). Due to FA's divalent chelating ability, this mycotoxin affects proteins that encompass divalent ions such as zinc finger proteins involved in DNA repair. FA has also been reported to impair protein synthesis (Bharathiraja *et al.*, 2010). Furthermore, an *in vivo* study reported tumouricidal activity of FA on head and neck squamous cancer cells following daily intra-lesional administration for a period of one month (Bharathiraja *et al*,. 2010). In young swines, FA showed moderate toxicity and induced vomiting and increased brain concentration levels of tryptophan and serotonin (Smith, 1992). Impaired regulation of serotonin synthesis caused elevated levels of this neurotransmitter; consequently, amplifying behaviours distinctive of the firing of serotonergic neurons such as loss of appetite and lethargy (Smith, 1992). In addition, FA decreased norepinephrine levels in the brain, heart, spleen and adrenal gland of rats (Terasawa and Kameyama, 1971).

2.1.3.3. In humans

In patients, FA was administered as a hypotensive agent but was discontinued due to noticeable hepatotoxicity (Wang and Ng, 1999). Recent preliminary studies showed cytotoxic effects of FA on WI-38 cells (fibroblastic cell line), LoVo cells (colorectal adenocarcinoma cell line) and MDA-468 cells (human breast adenocarcinoma cell line). FA inhibited the growth of WI-38 and LoVo cells at a concentration of 500 µM in a time and dose dependent manner (Fernandez-Pol, 1998). Following the removal of FA, 125 hours after treatment, growth of WI-38 and LoVo cells had resumed, suggesting that the majority of cells were arrested in G_1 (G_o) phase of the cell cycle. However, it was noted that after removal of FA approximately 95% of WI-38 cells had survived whilst there was almost an 80% decline in LoVo cells. This indicates a greater sensitivity of LoVo cells to FA compared to WI-38 cells. FA rapidly decreased MDA-468 cell numbers when treated with the same conditions as WI-38 and LoVo cells. After a 48 hour exposure, approximately 10% of the MDA-468 cells survived and continued to decline at greater exposure lengths (Fernandez-Pol, 1998). In addition, preliminary

findings showed the anti-viral potential of FA and had documented the reduction of retroviral mRNA expression levels (Fernandez-Pol, 1998).

2.2. The immune system

The immune system is one of the most vital systems of the body and is responsible for eliminating pathogens and dead and cancerous cells (Zarzycki and Tuszyńska, 2013). The immune system contains a diverse population of cells that remain in a dormant or inactive state (Pearce E.L and Pearce E.J, 2013). However, upon infection, inflammation or other perturbations, these cells become activated and rapidly respond to the site of infection (Pearce E.L and Pearce E.J, 2013). In order to perform its functions properly, these responses are regulated by specific cell types that activate or inhibit receptors that are responsive to pathogen-derived or intrinsic signals (Pearce E.L and Pearce E.J, 2013).

The immune system can be divided into two distinct, yet integrated systems. These include the innate and adaptive immune systems (Pearce E.L and Pearce E.J, 2013). The innate immune system is activated in response to pathogen entry, or upon recognition of injured or cancerous cells (Pearce E.L and Pearce E.J, 2013); and its defense mechanisms are characterized by a generic response with no long-term memory (Zarzycki and Tuszyńska, 2013). The adaptive immune system is highly specific and requires antigen presentation to distinguish between self and non-self (Zarzycki and Tuszyńska, 2013). The efficacy of the adaptive immune system is due to its immunological memory (Zarzycki and Tuszyńska, 2013).

These immune cell types of the innate and adaptive immune systems are derived from the thymus or bone marrow (Zarzycki and Tuszyńska, 2013). The thymus is responsible for the maturation of T lymphocytes and the cells developed from here are referred to as the lymphoid lineage (Zarzycki and Tuszyńska, 2013). The bone marrow gives rise to the myeloid lineage and includes erythrocytes, platelets, granulocytes, B lymphocytes, monocytes, and macrophages (Figure 1.3) (Zarzycki and Tuszyńska, 2013).

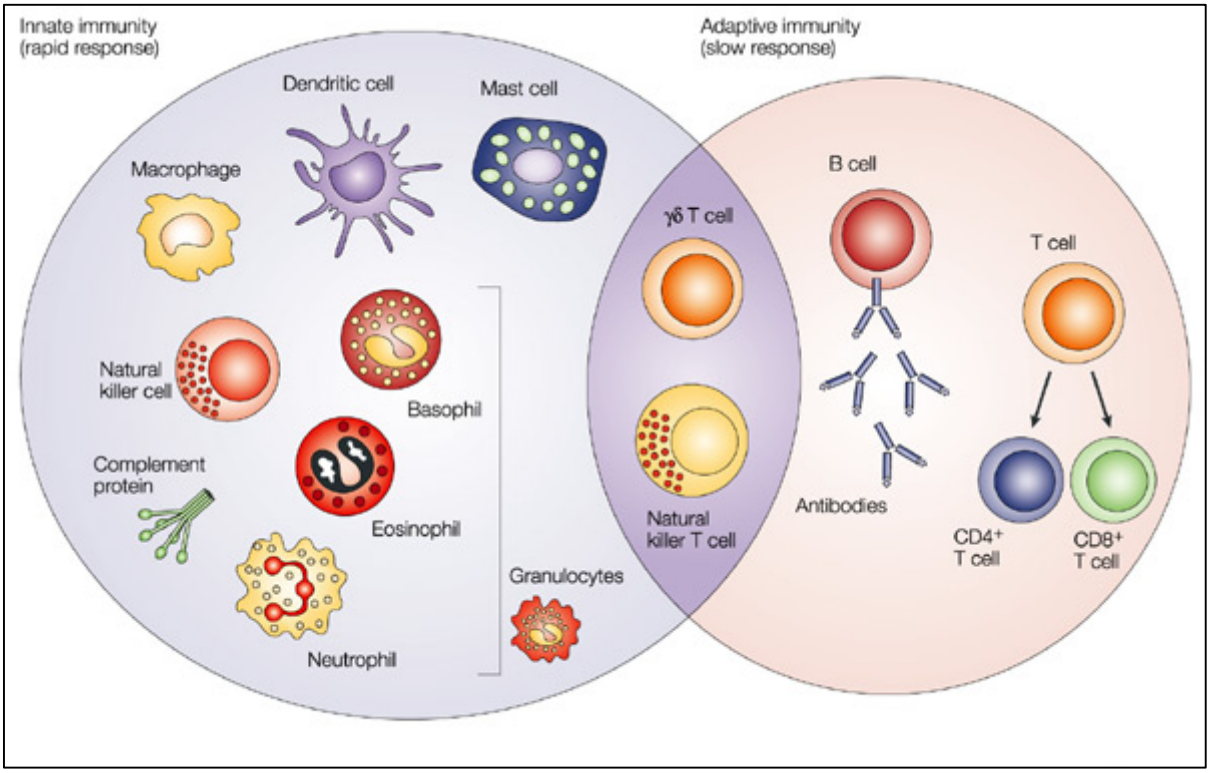

Figure 1.3: Immune cells involved in innate and adaptive immunity. (Zarzycki and Tuszyńska, 2013).

2.2.1. Peripheral Blood Mononuclear Cells

Peripheral Blood Mononuclear Cells (PBMCs) are a population of immune cells in blood that include lymphocytes (T cells- 45-70%; B cells-5-20%, NK cells-5-20%), monocytes (10-30%) and dendritic cells (1-2%) (Sanguine Biosciences, Inc., 2013). T cells can be classified as CD4 T cells and CD8 T cells (Figure 1.3). These types of T cells can exist as naïve, antigen experienced central memory or effector memory in dormant or activated states. CD4 T cells, also known as helper T (Th) cells can be further subdivided into regulatory T cells (Treg), Th1, Th2, and Th17. Th1 cells are activated mainly in response to intracellular pathogens, whereas, Th2 and Th17 counter host defense and bacteria, respectively (Sanguine Biosciences, Inc., 2013).

2.2.2. Thp-1 cell line

The Thp-1 cell line is a human acute monocytic leukaemia cell line, derived from a 1-year old male patient with acute monocytic leukaemia (Adati *et al.*, 2009). Monocytes represent a large proportion of leukocytes and are central players in the development and homeostasis of all organ systems in the body (Auffray *et al.*, 2009). They are structured with a group of receptors that identify and remove

toxic compounds, microorganisms and apoptotic cells (Auffray *et al.,* 2009). The Thp-1 cell line appear as large round cells in suspension (Adati *et al.,* 2009). Additionally, monocytes belong to the myeloid lineage and thus, have the ability to differentiate into macrophages, playing an important role in innate immunity (Auffray *et al.,* 2009). Thp-1 cells also have the ability to differentiate into macrophages upon stimulation with phorbol 12-myristate 13-acetate (PMA) (Adati *et al.*, 2009). Once differentiated, they resemble and behave like inborn monocyte derived macrophages (Adati *et al.*, 2009). Due to these characteristics, the Thp-1 cell line is not only used as a model for acute myeloid leukaemia, but also as a scientific model for immune response and macrophage differentiation (Adati *et al.*, 2009).

2.3. Cell death

Cell death can occur actively and passively (Auffray *et al.,* 2009). Active cell death, also known as programmed cell death (PCD), is important during development and tissue homeostasis and has been grouped into three types; namely, apoptosis (type I PCD), autophagy (type II PCD) and paraptosis (type III PCD) (Auffray *et al.,* 2009). Necrosis is a passive cell death affecting a large fraction of cells and is usually uncontrolled (Elmore, 2007).

2.3.1. Necrosis

Necrotic cell death is an energy-independent form of death and occurs upon a decrease in the energy supply of the cell and injury to cellular membranes (Elmore, 2007). Necrotic cells are distinguished by morphological features such as cell swelling, formation of cytoplasmic vacuoles and blebs, swollen endoplasmic reticulum; condensed, swollen or ruptured mitochondria, separation of ribosomes, damaged organelle membranes, swollen and ruptured lysosomes; and ultimately, injury of the cell membrane (Elmore, 2007). Alteration of cellular integrity results in the rupture of the cell membrane and the release of cytoplasmic contents. This induces chemotactic signals leading to the recruitment of inflammatory cells and the stimulation of an inflammatory response (Elmore, 2007). This form of cell death defers from apoptosis in that apoptotic cells do not release their cellular contents into the surrounding interstitial space and are engulfed by phagocytes preventing an inflammatory reaction (Elmore, 2007).

2.3.2. Apoptosis

Apoptosis is the best characterized type of PCD and is distinguished by distinct morphological features such as cell shrinkage, chromatin condensation, membrane blebbing, DNA fragmentation and other markers such as the externalization of phosphatidylserine on plasma membranes and the

activation of cysteine aspartate proteases (caspases) (Kaushik *et al.*, 2003; Auffray *et al.*, 2009). The externalization of phosphatidylserine acts as a cell surface marker for phagocytic cells to recognize and distinguish apoptotic cells from neighboring healthy cells, resulting in the clearance of apoptotic cells with minimum destruction of surrounding tissue and avoiding an inflammatory response (Elmore, 2007). Caspases are proteolytic enzymes that cleave aspartic acid residues on proteins (Elmore, 2007). Mammalian caspases can be grouped into initiator (caspases 2, 8, 9, 10) and effecter (caspases 3, 4, 6, 7, 11, 12, 13) caspases and their activation is a key event in the induction of apoptosis (Kaushik *et al.*, 2003). The biochemical activation of apoptosis occurs through two main pathways, the intrinsic apoptotic pathway and the extrinsic apoptotic pathway (Auffray *et al.*, 2009).

2.3.2.1. Intrinsic apoptotic pathway

The intrinsic apoptotic pathway is activated in response to several non-receptor mediated factors such as radiation, toxins, hypoxia, hyperthermia, viral infections, and free radicals (Elmore, 2007; Adati *et al.*, 2009). The execution of intrinsic apoptosis occurs via the mitochondrion which is tightly regulated by Bcl-2 family proteins (Hemmati *et al.*, 2002; Wan *et al.*, 2008). The Bcl-2 family entails both pro- and anti- apoptotic proteins which control the permeability and integrity of the mitochondrial membrane (Wan *et al.*, 2008; Adati *et al*., 2009). Pro-apoptotic proteins (BH3-only subfamily) include Bax, Bak, Bid, Bad, Bim, Noxa and Puma and anti-apoptotic proteins Bcl-2, Bcl-x, Bcl-XL, Bcl-XS (Wan *et al.*, 2008; Adati *et al.*, 2009). Upon apoptotic insults, one or more pro-apoptotic proteins are transcribed in the nucleus where they then translocate and bind to anti-apoptotic proteins located on the outer mitochondrial membrane (Wan *et al.*, 2008). This binding inhibits the activity of the anti-apoptotic protein leading to the opening of mitochondrial permeability transition pores (mPTP), alteration of the mitochondrial membrane potential and the release of pro-apoptotic proteins cytochrome c and Smac/DIABLO (Elmore, 2007). In turn, cytochrome c forms a complex with Apaf-1 and pro-caspase 9, known as the apoptosome (Elmore, 2007; Lui *et al*., 2000). The formation of the apoptosome activates caspase 9 which subsequently activates executioner caspases leading to the induction of apoptosis (Hemmati *et al.*, 2002; Lui *et al*., 2000) (Figure 1.4). The release of Smac/DIABLO inhibits the activity of inhibitor of apoptosis proteins (IAP) thereby amplifying apoptotic signaling (Elmore, 2007).

2.3.2.2. Extrinsic apoptotic pathway

The extrinsic apoptotic pathway initiates apoptosis in response to transmembrane receptor-mediated responses (Elmore, 2007). These receptors include FasL/FasR, TNF-α/TNFR1, Apo3L/DR3, Apo2L/DR4 and Apo2L/DR5 (Elmore, 2007). The tumor necrosis factor-α/tumor necrosis factor receptor 1 (TNF-α/TNFR1) is one of the best characterized receptors and is a key player in the transduction of

death signals from the cell surface to intracellular signaling pathways (Elmore, 2007). Upon binding of the ligand (TNF-α) to the receptor (TNFR1), a cytoplasmic adapter protein, TNF-α receptor associated death domain (TRADD), is recruited and binds to the receptor along with the recruitment of Fas-associated death domain (FADD) and the receptor-interacting serine/threonine kinase (RIP) (Elmore, 2007; Adati *et al.*, 2009). The receptor utilizes the adaptor molecules for the recruitment of initiator caspases (Adati *et al.*, 2009). FADD associates with pro-caspase 8 via dimerization, resulting in the formation of a death inducing signaling complex (DISC) where the pro-caspase is activated upon auto-catalytic cleavage (Elmore, 2007; Adati *et al.*, 2009) Activated caspase 8 then cleaves and activates effector caspases 3/7 leading to the execution of apoptosis (Elmore, 2007; Adati *et al.*, 2009; Lui *et al.*, 2000) (Figure 1.4).

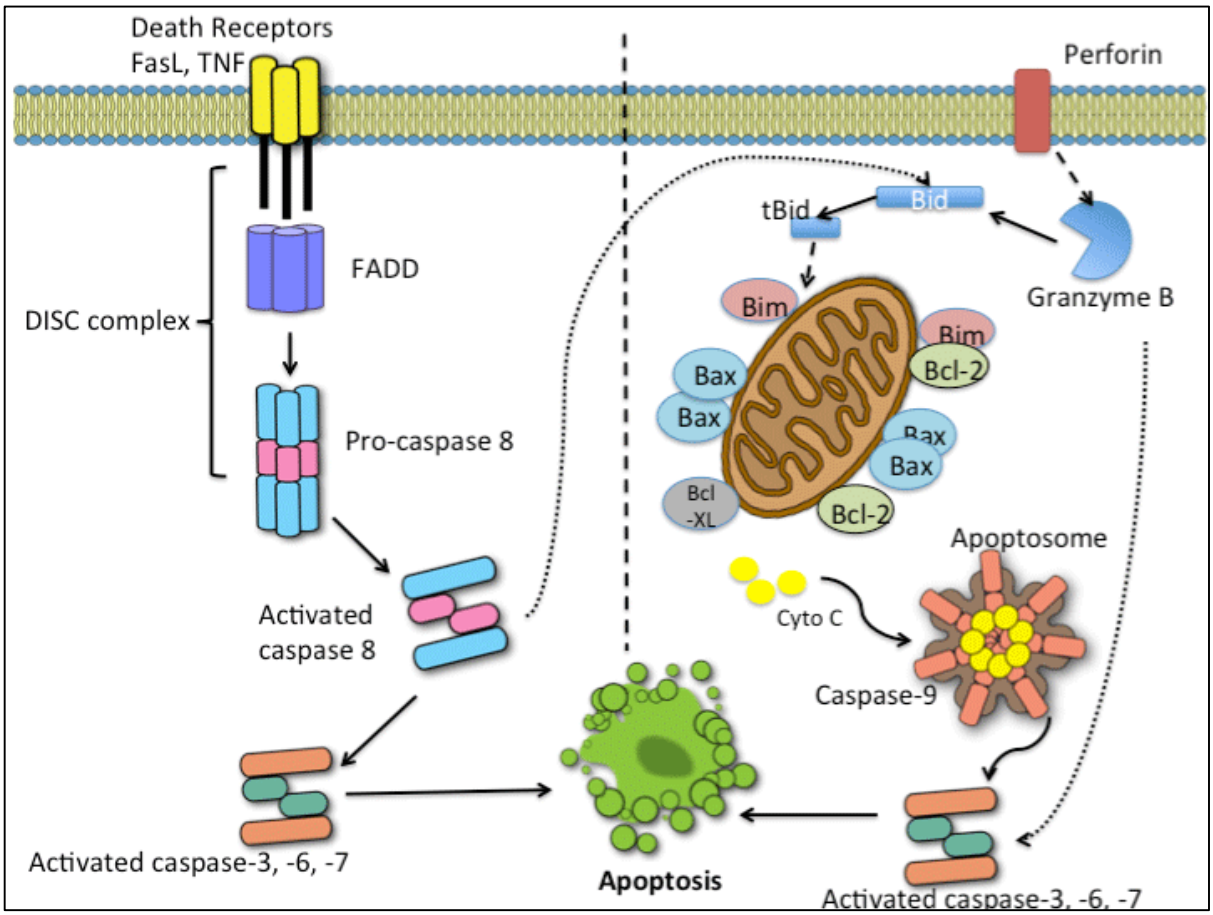

Figure 1.4: Intrinsic and Extrinsic apoptotic pathway. (Dawn, 2012).

2.3.3. Paraptosis

Paraptosis is a form of cell death distinct from necrosis and apoptosis. It is morphologically distinguished by cytoplasmic vacuolation, mitochondrial swelling, phosphatidylserine externalization, caspase independence and the absence of apoptotic features such as membrane blebbing, DNA fragmentation and apoptotic bodies (Auffray *et al*., 2009; Marchi *et al*., 2011; Sperandio *et al*., 2004). A study conducted by Sperandio and co-workers (2000) showed that activation of the insulin-like growth factor I receptor (IGFIR) induced paraptosis in human embryonic kidney (293T) cells and Apaf-1 null mouse embryonic fibroblasts following treatment with actinomycin D and cycloheximide. The authors alliterated morphological features and caspase independence seen in paraptosis. Although the biochemical activation of paraptosis remains relatively unknown, a study reported the involvement of tyrosine kinase and MAPKs in the induction of paraptosis by IGFIR and hesperidin, respectively, suggesting the association of signaling cascades in the initiation of paraptosis (Auffray *et al.*, 2009; Sperandio *et* al., 2004; Yumnam *et al.*, 2014).

2.4. Oxidative stress

Oxidative stress is defined as an imbalance in the equilibrium between free radicals and ROS produced in a cell and the ability of anti-oxidant systems to detoxify the reactive species (Dayem *et al.*, 2010; Son *et al.*, 2011). ROS are continuously produced by several cellular processes, with a significant amount generated as a by-product of aerobic respiration (Son *et al*., 2011; Barrera, 2012). In addition, ROS can be produced by other sources such as the endoplasmic reticulum (ER) and lysosomes (Son *et al*., 2011) (Figure 1.5). A substantial amount of ROS can also be generated by inflammatory processes, ionizing radiation, and chemotherapeutic agents (Son *et al.*, 2011). ROS include superoxide anion ($O2^{-\bullet}$), perhydroxyl radical ($HO_2^{\bullet}$), hydroxyl radical ($^{\bullet}OH$), nitric oxide (NO), hydrogen peroxide (H_2O_2), hypochlorous acid (HOCl), and peroxynitrite ($ONOO^-$) (Barrera, 2012). Excessive intracellular ROS levels can alter cellular functioning through oxidative damage of macromolecules such as DNA, proteins and lipids, which can cause certain human pathologies and cell death (Son *et al*., 2011; Barrera, 2012).

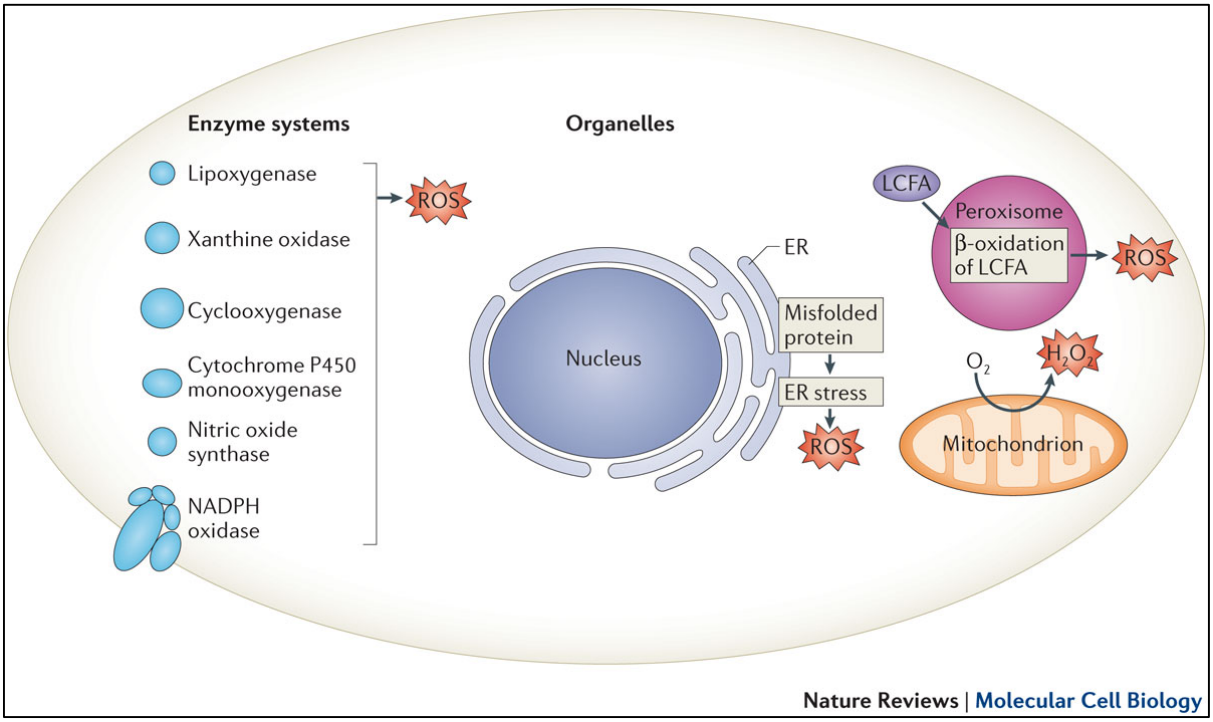

Figure 1.5: Sources of ROS in a cell. (Holmström and Finkel, 2014).

2.4.1. Mitochondrial production of ROS

The mitochondrion is a central player in aerobic respiration, an important biochemical process required for normal cellular function (Kuznetsov *et al.*, 2011). Mitochondria also participate in other cellular functions such as the induction of the intrinsic apoptotic pathway and maintaining cellular calcium and redox homeostasis (Kuznetsov *et al.*, 2011). Significant amounts of cellular ROS are generated by the mitochondria as a result of oxidative phosphorylation in the electron transport chain (ETC) (Gutterman, 2005; Dayem *et al.*, 2010). The ETC, located in the inner mitochondrial membrane, is responsible for ATP synthesis (Harper *et al.*, 2004). It entails the transfer of electrons through the chain of complexes from electron carries (Marchi *et al.*, 2011). These electron carriers are the reducing equivalents NADH and $FADH_2$ generated from the Krebs cycle (Marchi *et al.*, 2011). NADH enters at complex I and donates its electrons to the complex via oxidation to NAD^+. This reaction is catalyzed by the enzyme NADH dehydrogenase (Marchi *et al.*, 2011). At complex II, succinate dehydrogenase oxidizes $FADH_2$ to FAD (Marchi *et al.*, 2011). The electrons donated by NADH and $FADH_2$ at complexes I and II respectively, are transferred to complex III by the coenzyme ubiquinone (Marchi *et al.*, 2011). Cytochrome c oxidoreductase, the functional enzyme at complex III, transfers the electrons from ubiquinone to cytochrome c (Marchi *et al.*, 2011). Cytochrome c then travels to complex IV and attaches itself to a subunit in the complex (Marchi *et al.*, 2011). Thereafter, cytochrome oxidase reduces one oxygen molecule with two hydrogen ions producing one water

molecule (Marchi *et al.*, 2011). The resultant electron flux through the complexes, hyperpolarizes the inner mitochondrial membrane by the movement of hydrogen ions across each complex (Gutterman, 2005). This proton motive force drives the activity of adenine nucleotide transporter (ANT - complex V), in which ATP synthase phosphorylates adenosine diphosphate (ADP) to ATP (Harper *et al.*, 2004) (Figure 1.6).

Majority of ROS generated in the mitochondria occurs during the reduction of oxygen (molecular oxygen → superoxide anion → hydrogen peroxide → hydroxyl radical → water) (Marchi *et al.*, 2011). Superoxide anion acts as a precursor of most ROS and is generated both enzymatically by NADPH oxidase, cytochrome P_{450} oxygenases and xanthine oxidase and, non-enzymatically by the transfer of an electron to molecular oxygen (Marchi *et al.*, 2011). Additionally, superoxide anion reacts with other free radicals such as nitric oxide forming reactive nitrogen species (RNS) (Marchi *et al.*, 2011). The spontaneous or enzymatic (by superoxide dismutases - SODs) dismutation of superoxide anion results in the formation of hydrogen peroxide (Marchi *et al.*, 2011). Hydrogen peroxide is membrane permeable and can therefore diffuse into the cytosol where it can be removed by cytosolic or mitochondrial anti-oxidant systems (Marchi *et al.*, 2011). Superoxide anion can dissociate into hydroxyl radicals catalyzed by metal ions generated by the Fenton reaction (Marchi *et al.*, 2011). The free radical is highly reactive and acts as an oxidizing agent causing damage to cellular organelles (Marchi *et al.*, 2011). Complex I and III of the ETC are the two main sites responsible for the production of superoxide anions (Harper *et al.*, 2004). However, the degree of superoxide production is significantly accelerated by a decrease in oxygen consumption, a high proton gradient and a reduction in the ETC activity (Harper *et al.*, 2004).

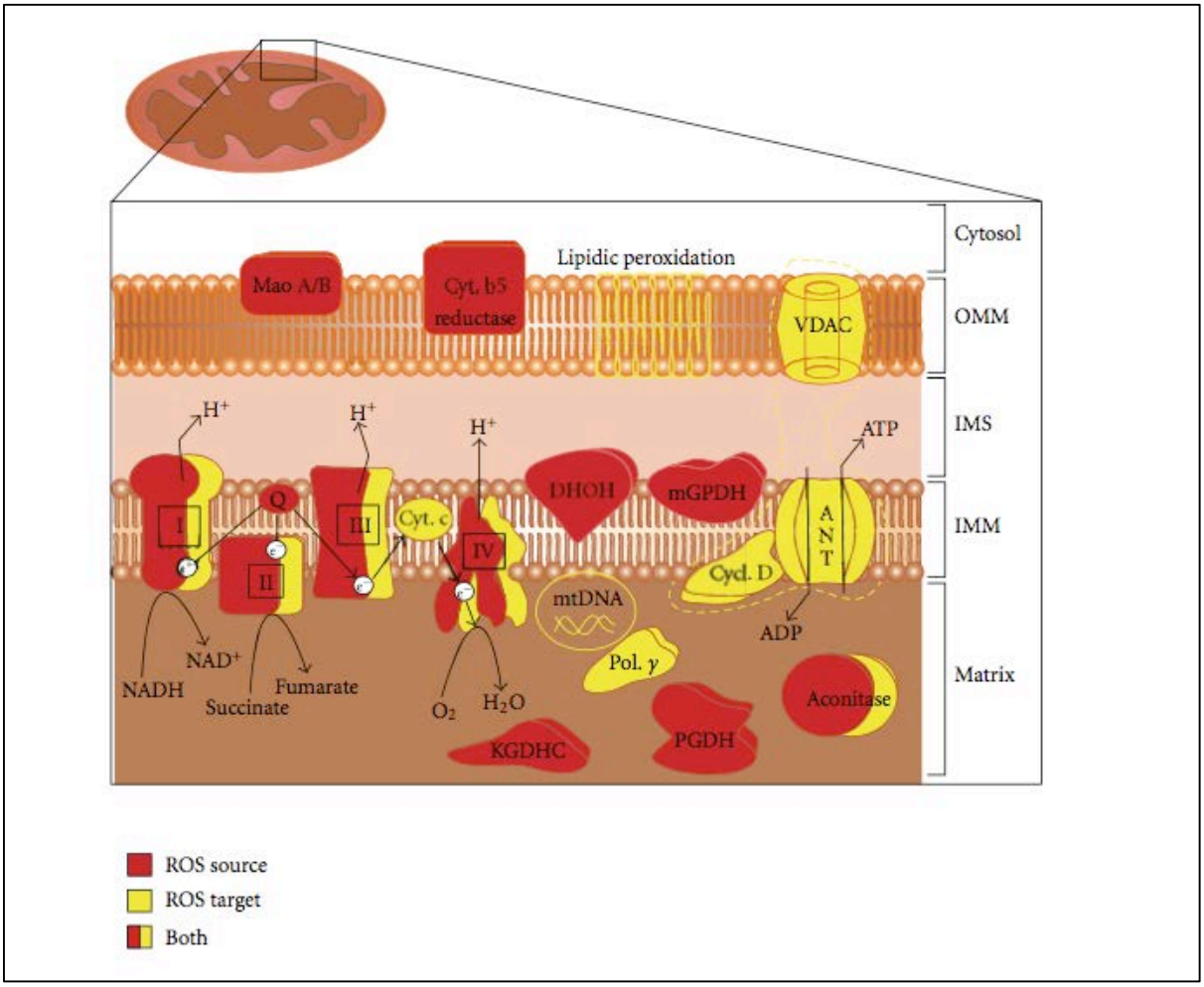

Figure 1.6: Sources of ROS production and targets in the mitochondria. (Marchi *et al*., 2011).

2.4.2. Lipid peroxidation

The initiation of lipid peroxidation occurs when reactive species, generated during oxidative stress, oxidize polyunsaturated fatty acids (PUFA) present in membranes (Marchi *et al*., 2011). PUFA are highly susceptible to hydroxyl radicals and result in the formation of a lipoperoxyl radical (Barrera, 2012). Subsequently, this radical reacts with a lipid producing a new lipid radical and an unstable hydroperoxide (Barrera, 2012). In turn, hydroperoxides yield highly reactive unsaturated aldehydes such as 4-hydroxy 2-nonenal (4-HNE), malondialdehyde (MDA) and acrolein (Marchi *et al*., 2011). Additionally, the production of lipid radicals may initiate a chain reaction resulting the in the formation of new lipid radicals intensifying the peroxidation of lipids (Marchi *et al*., 2011). Lipid peroxidation of the inner mitochondrial membrane increases the permeability to protons and the uncoupling of oxidative phosphorylation (Marchi *et al*., 2011). Cardiolipin, an abundant unsaturated fatty acid present in the mitochondrial membrane, affects the functioning of cytochrome c oxidase (complex IV) and ANT thereby decreasing ATP production (Harper *et al*., 2004). Furthermore, lipid

radicals can easily diffuse into the mitochondrial membrane and covalently bind to proteins resulting in membrane depolarization and an impaired mitochondrial function (Harper *et al*., 2004; Marchi *et al*., 2011). However, oxidative stress not only affects the mitochondria, but also extra-mitochondrial components such as DNA, proteins and membrane lipids, dramatically altering cellular integrity leading to cell death (Harper *et al*., 2004; Dayem *et al*., 2010).

2.4.3. ROS as a second messenger

The advancement that mitochondrial function expands further than ATP synthesis and that ROS is not only injurious to cells but may also mediate cell signaling pathways has unlocked new research outlooks in biology (Gutterman, 2005). The amount of intracellular ROS has a significant influence on many signaling pathways such as the MAPK and Akt cascades (Kim *et al*., 2014). For example, mitochondrial-derived hydrogen peroxide, can act as a second messenger in the cytosol mediating processes such as stress response, metabolism, cell cycle regulation and redox homeostasis (Marchi *et al*., 2011; Kim *et al*., 2014).

2.5. Mitogen Activated Protein Kinases (MAPKs)

Mitogen-activated protein kinases (MAPKs) are a family of proline-directed, serine/threonine kinases important in regulating cellular processes such as proliferation, differentiation, metabolism, cell death, cell-to-cell interaction, inflammatory responses and gene expression (Dhillon *et al.*, 2007; Cuenda and Rousseau, 2007; Son *et al.*, 2011). The transduction of extra- and intra-cellular signals to the nucleus occurs via sequential phosphorylation of MAPKs (Kondoh *et al.*, 2005). In mammalian cells, there are three well-characterized groups of MAPKs: the extracellular signal-regulated kinase (ERK), c-Jun N-terminal kinase (JNK), and p38 kinase (Dhillon *et al*., 2007; Zhang and Liu, 2002). Essential for MAPK activation, are a three-tiered kinase module composed of a MAPK kinase kinase (MAPKKK), a MAPK kinase (MAPKK) and a MAPK (Boldt *et al*., 2002; Cuenda and Rousseau, 2007; Dhillon *et al*., 2007). The first component activated in the MAPK module is the MAPKKKs. In response to stimuli, MAPKKKs interact with small GTP-binding proteins of the Ras/Rho family and undergo phosphorylation thereby activating the kinase (Zhang and Liu, 2002). MAPKKKs have specific motifs in their sequences that determines the selectively of phosphorylation and activation of MAPKKs in response to different stimuli (Cuenda and Rousseau, 2007). In turn, MAPKKs activate MAPKs through dual phosphorylation on both threonine and tyrosine residues located within the activation loop of the kinase subdomain VIII (Zhang and Liu, 2002). Activation of specific MAPKs is due to the interaction between the N-terminal region located on the MAPKK and the docking site located on the MAPK, as well as the phosphorylation motif located in the activation loop of the MAPK (Cuenda and Rousseau, 2007). The docking site entails the threonine-X-tyrosine sequence,

where X represents an amino acid specific to MAPKKs (Cuenda and Rousseau, 2007). Activated MAPKs phosphorylate several substrates on serine or threonine residues, followed by a proline, that regulates the activity of transcription factors, phospholipases, cytoskeletal proteins and other kinases such as the mitogen-and-stress-activated kinase (MSK), the MAPK-interacting kinase (MNK) and the MAPK-activated protein kinase-2, -3 and -5 (MK-2, -3 and -5) (Zhang and Liu, 2002). The specificity of substrate activation is dependent on the interaction between the MAPK and the motifs present on the substrate (Zhang and Liu, 2002).

Two isoforms of ERK MAPK have been studied in detail. These include ERK1 and ERK2. The ERK signaling pathway is generally activated by MAP/ERK Kinase (MEK), which is activated by the MAPKKK, Raf (Son *et al.,* 2011; Zhang and Liu, 2002). The activation of MAPKKK occurs upon ligation and phosphorylation of stimuli on growth factor receptors (Dhillon *et* al., 2007; Son *et al.,* 2011). Recent studies demonstrated that the phosphorylation and activation of growth factor receptors was mediated by hydrogen peroxide thereby indicating ligand-independent activation of ERK activity (Son *et al.,* 2011) (Figure 1.7).

The JNK MAPK, also known as stress activated protein kinase (SAPK), includes isoforms JNK1, JNK2 and JNK3 and is activated in response to extracellular signals such as the ligation of cytokines on several receptors, and intracellular signals such as ROS generation, DNA damage, protein degradation and numerous other stress signals (Dhillon *et al.*, 2007; Son *et al.*, 2011) . The MAPKKs involved in the activation of JNK include MKK4 and MKK7 (Dhillon *et al*., 2007; Son *et al.,* 2011). Additionally, MKK4 can activate the MAPKKs (MKK3 and MKK6) implicated in p38 signaling (Son *et al.*, 2011) (Figure 1.7).

The p38 MAPK consists of p38-α, p38-β, p38-γ, and p38-δ isoforms (Dhillon *et al.*, 2007; Son *et al.*, 2011; Zarubin and Jiahuai, 2005). p38 signaling is generally activated in response to inflammatory cytokines, in addition to other stimuli such as osmotic stress, UV radiation, DNA damage and oxidative stress (Dhillon *et al.*, 2007; Son *et al.,* 2011; Zarubin and Jiahuai, 2005). The MAPKKs involved in the activation of p38 signaling are highly specific for p38 (Son *et al.,* 2011). These include MKK3 and MKK6. MKK6 is able to phosphorylate all isoforms of the p38 family. However, MKK3 is only able to phosphorylate p38-α, p38-γ, and p38-δ but not p38-β (Dhillon *et al.*, 2007; Son *et al.*, 2011). Several MAPKKKs such as MEKK1, -2, -3 and -4, mixed-lineage kinase (MLK), apoptosis signal-regulating kinase 1 (ASK1) and transforming growth factor β-activated kinase 1 (TAK1) can phosphorylate and activate both JNK and p38 MAPKKs (Son *et al.*, 2011) (Figure 1.7).

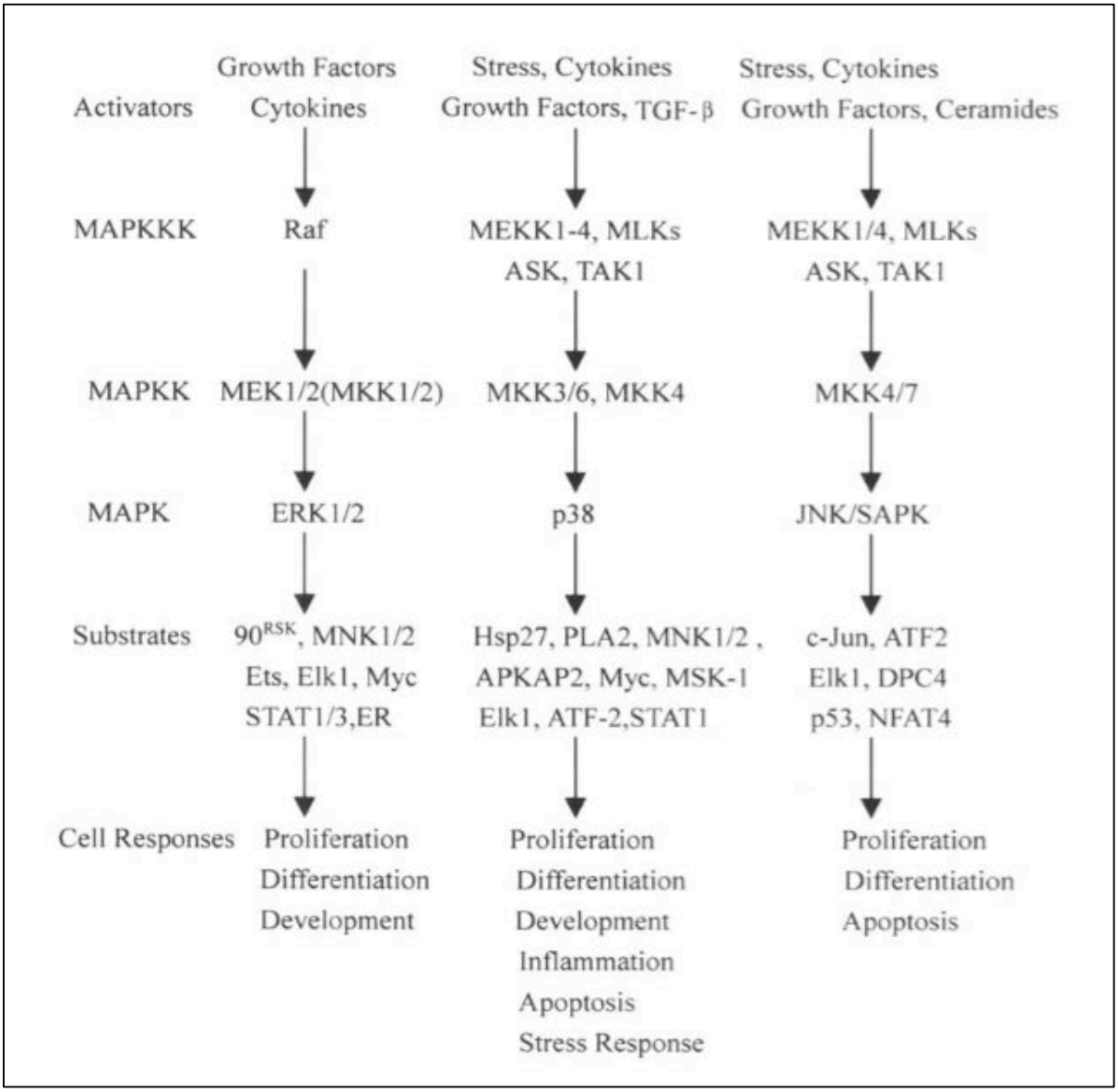

Figure 1.7: Summary of the conventional MAPK signaling cascade. (Zhang and Liu, 2002).

2.6. Protein Kinase B (Akt)

The serine/threonine protein kinase B (Akt) is a 56 kDa protein that was initially classified as a retroviral oncogene (Martelli *et al*., 2012). The kinase is a key player in regulating energy metabolism and promoting survival signals (Los *et al*., 2009; Zhang *et al*., 2013). In addition, Akt signaling influences apoptotic cell death and tumor-related diseases via activation of downstream signaling molecules (Los *et al*., 2009; Zhang *et al*., 2013). The structure of the protein is composed of a catalytic domain, a C-terminus regulatory domain and an N-terminus pleckstrin homology (PH) domain (Martelli *et al*., 2012). Activation of Akt occurs downstream of the kinase phosphatidylinositol 3-kinase (PI3K) (Los *et al*., 2009). Upon extracellular stimuli, such as growth

factors and cytokines, PI3K synthesizes phosphatidylinositol 3,4,5- triphosphate (PIP3) leading to the recruitment and binding of Akt to PIP3 via the N-terminus PH domain (Martelli *et al*., 2012). The resultant binding phosphorylates Akt at threonine 308 ($pAKT^{Thr308}$) and serine 473 ($pAKT^{Ser473}$) residues activating the kinase (Nogueira *et al*., 2008). Once activated, Akt translocates to the nucleus or other organelles including the mitochondria and endoplasmic reticulum where it phosphorylates or interacts with other cellular components (Martelli *et al*., 2012). In contrast to Akt's survival signaling properties, hyperactivation of the kinase increases ROS production and thus oxidative stress (Cuenda and Rousseau, 2007). One of the substrates targeted by Akt is the Forkhead (FOXO) family transcription factors. FOXO transcription factors up-regulate the expression of antioxidant proteins and thus protect the cell from oxidative damage (Cuenda and Rousseau, 2007). Inhibition of FOXO transcription factors, following phosphorylation by Akt, renders the cell susceptible to oxidative-induced cell death (Cuenda and Rousseau, 2007). Thus, Akt has a role in regulating both cell survival and cell death (Nogueira *et al*., 2008).

CHAPTER 2

MATERIALS AND METHODS

2.1. Materials

Cell culture reagents for PBMC maintenance were purchased from Sigma Aldrich. The Thp-1 cells and media were purchased from ATCC (University Boulevard Manassas, USA) and Scientific group (Johannesburg, SA), respectively. FA (*Gibberella fujikuroi*) was purchased from Sigma Aldrich.

2.2. Isolation and maintenance of Peripheral Blood Mononuclear Cells

PBMCs were isolated from whole blood from young healthy Asian males following institutional ethical approval (BE057/15) and written informed consent. An equal volume of blood was layered onto 5 ml Histopaque 1077 (Sigma) in 15 ml sterilin tubes. The sterilin tubes were then centrifuged (400 xg, 30 minutes (min), 24 ºC). Afterwards, the serum was aspirated and discarded. The buffy coat containing PBMCs was aspirated and washed once in 0.1 M phosphate buffer saline (PBS) (Figure 2.1). The PBMCs were re-suspended in RPMI 1640 medium supplemented with 10% foetal calf serum (FCS), 1% L-glutamine and 1% pencillin-streptomycin. The cells were maintained in 75 cm^3 ventilated flasks [(37 ºC with 5% carbon dioxide (CO_2)]. Viability of cells was assessed using trypan blue exclusion.

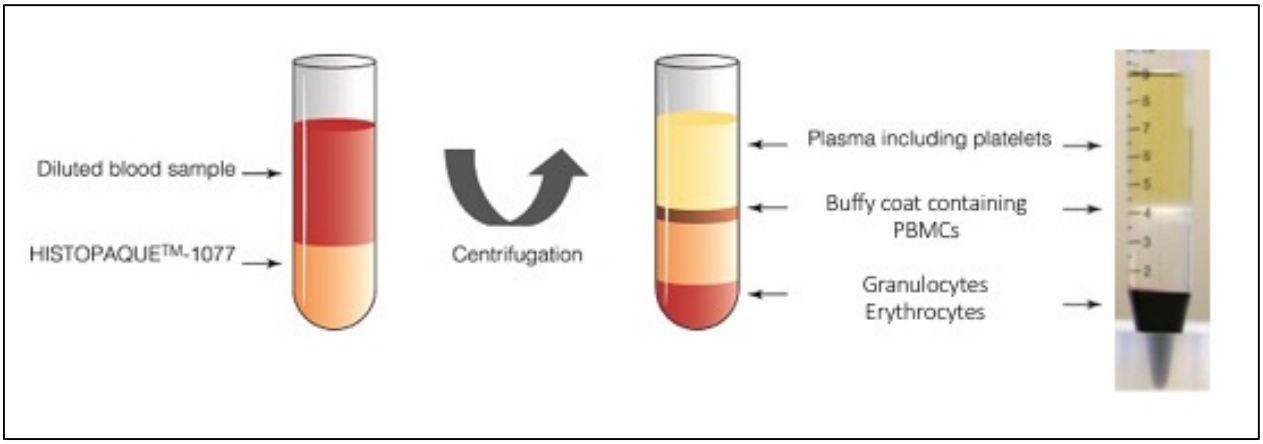

Figure 2.1: Isolation of PBMCs from whole blood using gradient centrifugation. (Prepared by author).

2.3. Thp-1 cell culture

The Thp-1 cells were cultured in RPMI 1640 medium supplemented with 10% FCS, 1% L-glutamine, 1% pencillin-streptomycin, 1 mM sodium pyruvate and 0.05 mM β-mecaptoethanol. The cells were maintained at 3 x10^5 cells/ml in 75 cm^3 ventilated flasks at (37 ºC, 5% CO_2) and were split at a cell count of 8 x10^5 cells/ml. Viability of cells was assessed using trypan blue exclusion.

2.4. Cell viability

2.4.1. WST-1 assay

The water soluble tetrazolium-1 (WST-1) assay was used to determine the immunotoxicity of FA on healthy PBMCs and Thp-1cells. The WST-1 reagent is a stable tetrazolium salt reduced by viable cells into a soluble formazan product. This reduction is dependent on the glycolytic production of NADPH in which the enzyme NADPH oxidoreductase, present in the cytosol, reduces NADH to NAD^+. Therefore, the intensity of the formazan dye formed is directly proportional to the number of metabolically active cells in the culture. The WST-1 reagent, however, carries a net negative charge and is therefore membrane-impermeable. Hence, the reduction of the anion occurs at the plasma membrane via trans-plasma membrane electron transport (Figure 2.2).

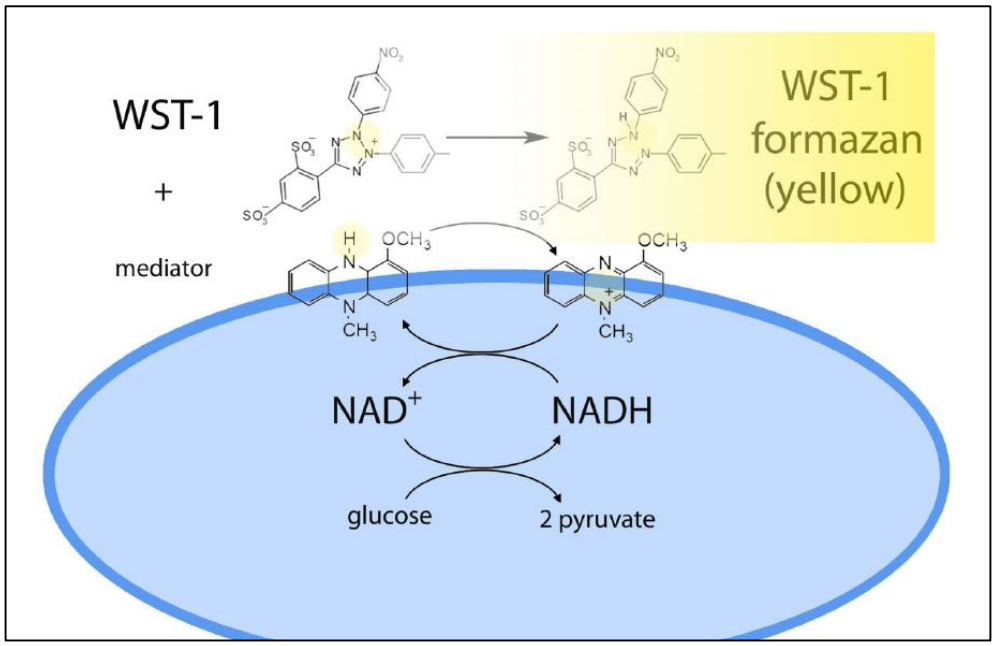

Figure 2.2: Reduction of WST-1 salt to a yellow formazan by a viable cell. (3D Biomatrix, 2015).

For the WST-1 assay, PBMCs and Thp-1 cells (20000 cells/ 100 µl well) were seeded into a 96-well microtitre plate. Varying treatment concentrations (25-300 µg/ml) were added to the cell suspension in triplicate (100 µl/well) and was incubated for 24 hours (hrs) (37 ºC, 5% CO_2) including a positive control of cells with RPMI only. Following incubation, the plate was centrifuged (24 ^{0}C, 400 xg, 10 min) and thereafter the supernatant was aspirated. Afterwards, 110 µl/well of a RPMI/WST-1 reagent solution (1:10) was added and incubated for 3 hrs (37 ^{0}C, 5% CO_2). A negative control with RPMI/WST-1 reagent solution was utilised. The optical density of the colorimetric reaction was measured at a wavelength of 450 nm and reference wavelength of 620 nm using a spectrophotometer (Bio-Tek uQuant). The results were expressed as percentage cell viability versus log FA concentration from which a half maximum inhibition (IC_{50}) was extrapolated using GraphPad Prism v5.0 software. The percentage cell viability was calculated as follows:

$$\% \text{ cell viability} = \frac{mean\ absorbance\ of\ treatment}{mean\ absorbance\ of\ control} \times 100$$

2.4.2. ATP levels

Adenosine triphosphate (ATP), a complex molecule, is the prime energy source in viable cells and is required for many cellular functions such as the transport of substances across membranes, heart and skeletal muscle contraction for blood circulation and body movement, macromolecule synthesis and the regulation of cell signaling.

Luminometry was performed to assess ATP levels using the ATP CellTitre Glo reagent (Promega). The ATP CellTitre Glo reagent is based on the firefly luciferase reaction in which beetle luciferin is mono-oxygenated to oxyluciferin. This reaction is catalysed by luciferase in the presence of ATP, magnesium and oxygen. Oxyluciferin releases energy in the form of light. The light emitted is detected by the luminometer and its intensity is related to the amount of ATP present in cells (Figure 2.3).

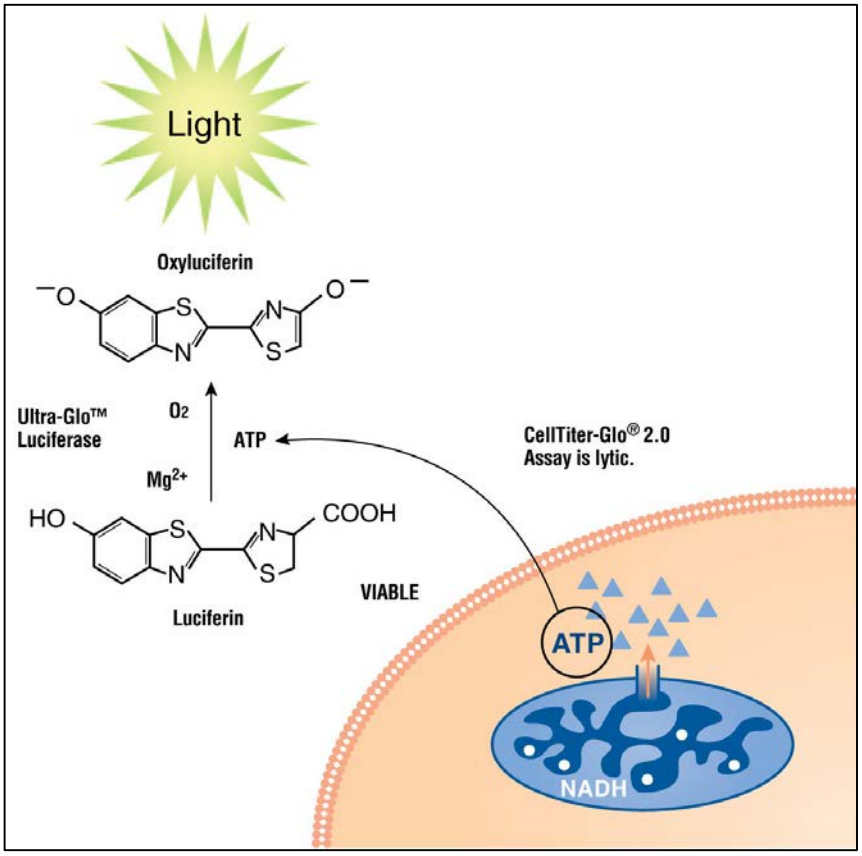

Figure 2.3: Principle of the CellTitre Glo ATP assay. (Promega Corporation, 2015).

Following treatment, 20 000 cells/well were seeded into a 96-well opaque polystyrene microtitre plate in triplicate. The ATP CellTitre Glo reagent (100 µl/well) was added to each sample and incubated in the dark for 30 min (RT). Thereafter, the luminescence was measured on a Modulus™ microplate luminometer. The data was expressed as relative light units (RLU).

2.5. Analysis of cell death parameters

2.5.1. Annexin V-FITC staining

In viable cells, the negatively charged phospholipid, phosphatidylserine, is located on the inner leaflet of the plasma membrane. Upon the induction of cell death, phosphatidylserine becomes externalised on the outer leaflet of the plasma membrane to allow for the removal of dying cells by phagocytic cells. This event is an early feature of apoptotic cell death. Annexin V is a 35 kDa protein with a high binding affinity for phosphatidylserine, in the presence of calcium. Annexin V can be conjugated with fluorochromes while maintaining its affinity for phosphatidylserine. Thus, this characteristic serves as an ideal probe for flow cytometric analysis of apoptotic cells. Annexin V can also be conjugated to

other dyes such as propidium iodide (PI). PI is membrane-impermeable and thus cells with intact membranes stain negative for PI. Loss of membrane integrity is a key feature of necrotic cell death and thus aids in distinguishing the mode of cell (Figure 2.4).

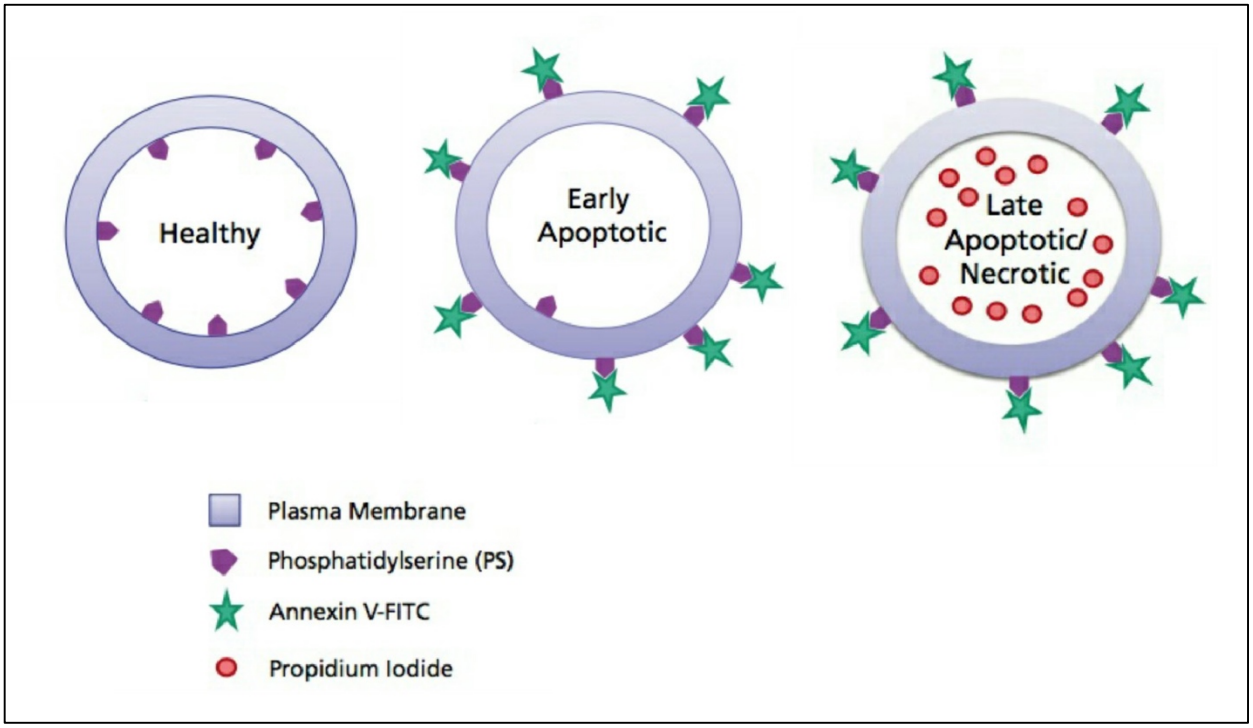

Figure 2.4: Principle of Annexin V-FITC and propidium iodide staining in the detection of apoptotic and necrotic cells. (BD Biosciences, 2011).

Flow cytometry was performed to determine the externalisation of phosphatidylserine. Following treatment, 100 µl of an Annexin V-FITC Fluos solution [1:1:50; annexin V-FITC: PI: staining buffer (Roche)] was added to each sample (200 000 cells in 100 µl PBS) and incubated in the dark (15 min, RT). Thereafter, the samples were analysed on the Accuri^{TM} C6 flow cytometer. A total of 20 000 events were analysed for apoptotic, necrotic and viable cells. The cells were gated to exclude cellular debris using the Accuri^{TM} C6 flow cytometer Fl-1 channel (525 nm) (Becton Dickinson). The results were expressed as a percentage.

2.5.2. Caspase activity

Caspase activation is a key event in the induction of apoptosis. The Caspase-Glo assay kit allows for easy detection of caspase activity using luminescence. Caspases contain a tetra-peptide sequence. This sequence is cleaved and acts as a substrate along with ATP, magnesium and oxygen for the luciferase

reaction. The amount of light emitted by the reaction is directly proportional to the caspase activity (Figure 2.5).

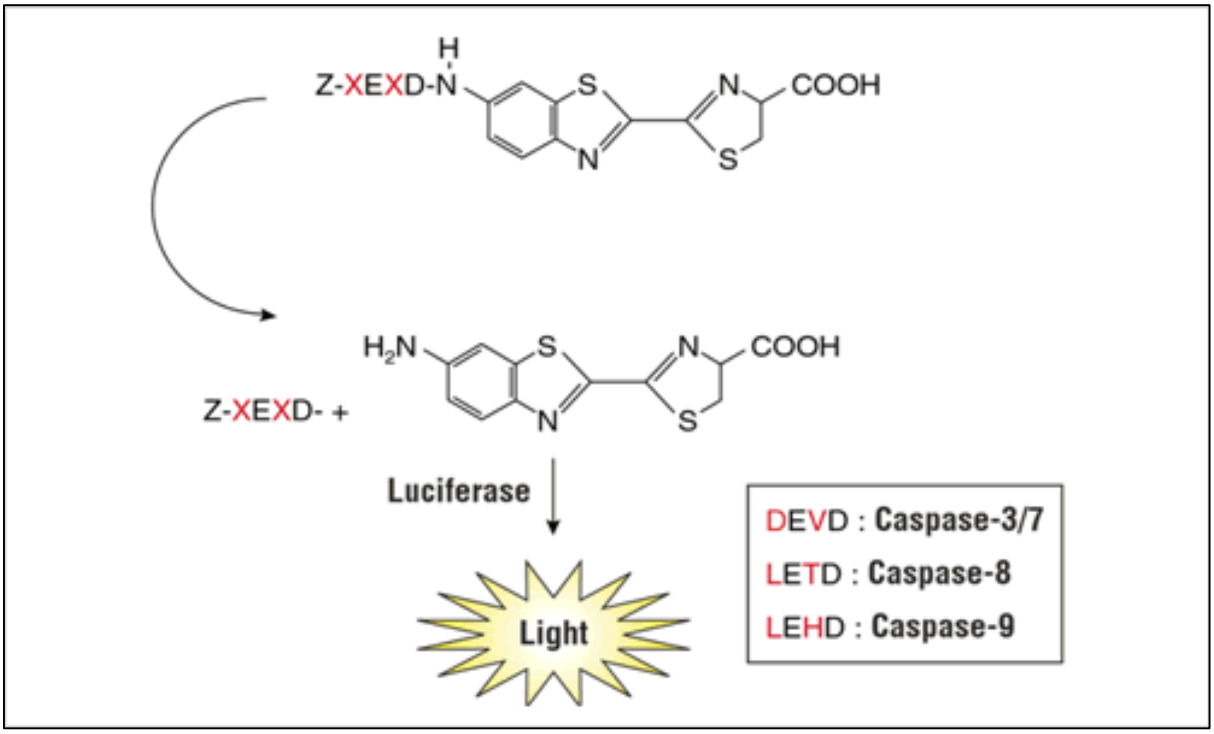

Figure 2.5: Principle for the detection of caspase activity. (Promega Corporation, 2015).

Luminometry was performed to assess caspase activities 8, 9 and 3/7. Approximately 20 000 cells/well (in 50 µl) were seeded into a 96-well opaque polystyrene microtitre plate in triplicate. Subsequently, 50 µl/well of the reagent [Caspase-Glo® 3/7, Caspase-Glo® 8 and Caspase-Glo® 9 Assays (Promega)] was added to each sample and incubated in the dark (30 min, RT). Thereafter, the luminescence was measured on a Modulus™ microplate luminometer. The data was expressed as relative light units (RLU).

2.5.3. Tumour necrosis factor-α

The enzyme-linked immunosorbent assay (ELISA) is based on antigen quantification between two layers of antibodies (i.e. capture and detection antibody). Proteins in a sample can competitively bind lowering the quantity of immobilized antigen. Therefore, the first layer consists of a capture antibody. The capture antibody is a specific antibody used to attach the antigen to the surface of the micotitre plate thereby increasing the specificity of the assay. Once the plate is coated with the capture antibody, the plate is blocked to reduce non-specific binding and is coated with the samples. Thereafter, the plate is coated with a substrate solution that is composed of an enzyme-linked

secondary antibody, such as horseradish peroxidase (HRP) that binds to the Fc region of the antigen. The conjugated enzyme produces a colorimetric reaction that is stopped by the addition of a stop solution containing sulphuric acid (H_2SO_4). The intensity of the reaction is directly proportional to the amount of the antigen of interest and is quantified using a spectrophotometer (Figure 2.6).

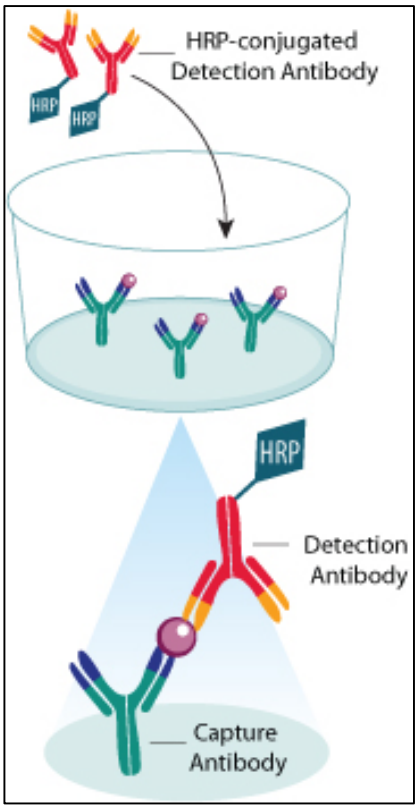

Figure 2.6: Sandwhich ELISA principle used to measure TNF-α levels. (R&D Systems, Inc., 2015).

To determine the effect of FA on TNF-α levels, the TNF-α ELISA kit (555212, BD Biosciences) was used. Microwells (96-well plate) were coated with 100 µl/well capture antibody and were incubated overnight at 4°C. Following incubation, the plate was washed three times with a 1X wash buffer (300 µl/well) and blocked with 200 µl/well assay diluent (1 h, RT). The plate was then washed three times with wash buffer (300 µl/well). Subsequently, 100 µl/well of each standard (eight standards of TNF-α were prepared as per manufactures instructions) and samples were aliquoted and incubated for 2 hrs (RT). Afterwards, the plate was washed five times with wash buffer (300 µl/well) and incubated with 100 µl/well working detector (prepared as per manufactures instructions) (1 hr, RT). After incubation, the plate was washed seven times with wash buffer (300 µl/well) and 100 µl/well of substrate solution was added and incubated in the dark (30 min, RT). Thereafter, 50 µl/well of a stop solution was aliquoted. The optical density was measured on a spectrophotometer (Bio Tek uQuant) at 450nm with

reference wavelength of 570nm. TNF-α concentration levels were extrapolated from the standard curve.

2.6. Oxidative stress

2.6.1 Lipid peroxidation

Peroxidation of lipids occur upon excessive amounts of reactive species produced by the electron transport chain in the mitochondrion. These free radicals oxidize PUFA due to the double hydrogen bonds present between adjacent carbon atoms resulting in a free radical chain reaction. This chain reaction yields lipid peroxides such as MDA and 4-HNE (Figure 2.7). The Thiobarbituric acid reactive substances assay (TBARS) measures the amount of MDA in a sample and thus is used as a marker of oxidative stress. The TBARS assay is based on the condensation of two molecules of the chromogenic reagent, 2-thiobarbituric acid, with one molecule of MDA. This reaction yields a chromophore (MDA-TBA adduct) that is detected at an absorbance wavelength of 532nm.

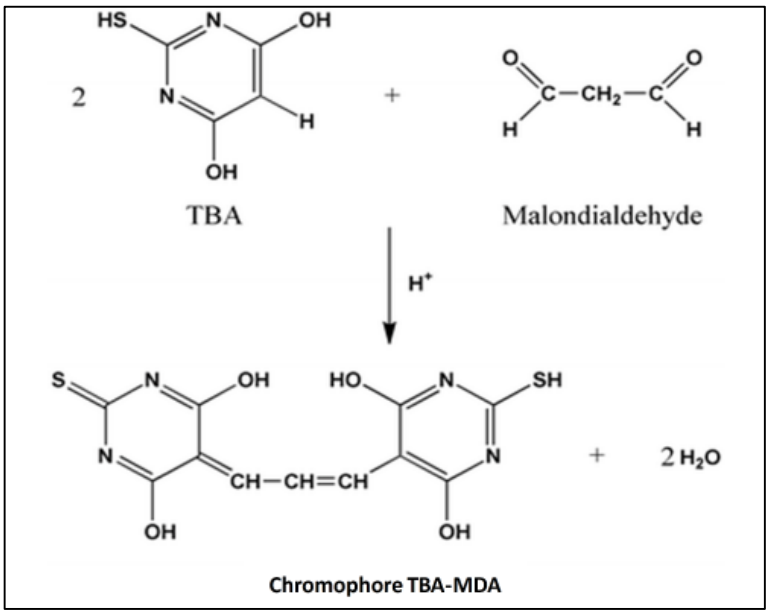

Figure 2.7: Principle of the TBARS assay. (Sochr *et al.*, 2014).

Briefly, 400 µl supernatant from each sample was transferred to a set of test tubes. Thereafter, 200 µl of 2% H_3PO_4, 400 µl of 7% H_3PO_4 and 400 µl of TBA/BHT solution were added to each sample. A positive control containing MDA (1 µl) and a negative control containing 3 mM HCl were prepared. All samples were vortexed and 200 µl of a 1 M HCl solution was added to each sample. Thereafter, the samples were heated in a water bath (100°C, 15 min) and allowed to cool (RT). After cooling, 1.5

ml butanol was added to each sample, vortexed and allowed to separate into distinct phases. Thereafter, 100 µl of the upper butanol phase from each sample was aliquoted into a 96-well microtitre plate in triplicate. The optical density was measured on a spectrophotometer (Bio Tek uQuant) at 532nm with reference wavelength of 600nm.The mean optical density for each sample was calculated and divided by the absorption coefficient (156 mM^{-1}). The results were expressed in µM.

2.6.2. Mitochondrial membrane potential

The mitochondrion plays an important role in the production of ATP, ROS and the induction of intrinsic apoptosis. Disruption of mitochondrial function is a key feature of programmed cell death. These modifications include alterations of mitochondrial membrane potential and the redox status of the mitochondria. The JC-1 stain is a positively charged monomer that is highly selective to the mitochondria. The stain can freely cross cell membranes and aggregate in the electronegative regions within the mitochondria due to a high affinity to lipophilic components and negative charges within the mitochondrial membrane. The electron gradient created during oxidative phosphorylation maintains the mitochondrial membrane potential at a polarized state. During this state, the dye aggregates in the mitochondrial membrane and emits a red fluorescence (Figure 2.8). Disruption of the electron gradient causes a collapse in the membrane potential and results in depolarization. At a depolarized state the dye remains in the cytoplasm and emits a green fluorescence (Figure 2.8).

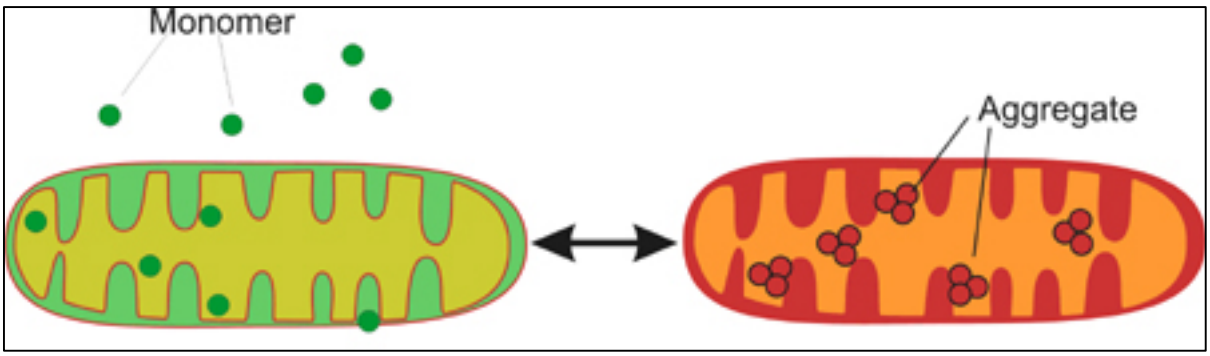

Figure 2.8: Spectral shift seen during mitochondrial polarization and depolarization using the JC-1 stain. (BioTek Instruments, Inc., 2015).

Flow cytometry was performed to determine mitochondrial membrane potential using the JC-1 Mitoscreen kit (BD Biosciences). Briefly, 100 µl of a JC-1 working solution was added to each sample (200 000 cells in 100 µl PBS) and incubated in the dark (30 min, RT). Following incubation, 100 µl flow cytometry sheath fluid was added to each sample and were analysed on the Accuri™ C6

flow cytometer. A total of 20 000 events were gated using Accuri™ C6 flow cytometer Fl-1 channel (525 nm) (Becton Dickinson). The results were expressed as a percentage.

2.7. Western blotting

Western blots were performed to analyse the protein expressions of p-Akt, p-ERK, p-JNK, p38, Bax and p-Bcl-2.

2.7.1. Protein isolation

Total protein was isolated using Cytobuster™ reagent (Novagen). Cells were re-suspended in 150 µl Cytobuster and incubated on ice (30 min). Following incubation, the cells were centrifuged (10 min, 180 xg, 4°C). The supernatant was aspirated and transferred into 1.5 ml eppendorfs and kept on ice until further use.

2.7.2. Protein quantification and standardisation

Proteins are composed of amino acids that are linked together by peptide bonds. The bicinchoninic acid (BCA) assay is based on the Biuret reaction in which copper ions (Cu^{2+}) react with the peptide bonds present in proteins and are reduced to cuprous ions (Cu^{+}). The formation of Cu^{+} forms a complex with two BCA molecules producing a purple colour under alkaline conditions (Figure 2.9). The intensity of the colour is directly proportional to the quantity of protein in a sample.

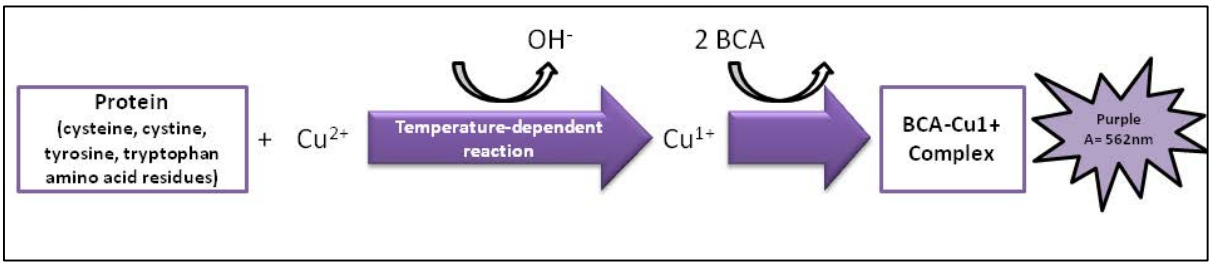

Figure 2.9: Principle of the BCA assay. (Microamaze, 2015).

Protein samples were quantified by the bicinchoninic acid assay and standardised to 0.2 mg/ml (PBMCs) and 1.0 mg/ml (Thp-1). The samples were then boiled (100 ^{0}C) in Laemmli Sample buffer (dH_20, 0.5M Tris-HCl (pH 6.8), glycerol, 10% SDS, β-mercaptoethanol, 1% bromophenol blue) for 5 min (100 ^{0}C), to allow proteins to unfold (Figure 2.10). Thereafter, the samples were stored at -20 ^{0}C until further use.

2.7.3. SDS-PAGE gel electrophoresis

Sodium dodecyl sulphate-polyacrylamide gel electrophoresis (SDS-PAGE) is a technique commonly used for the separation of protein based on the molecular weight and charge of the protein. SDS is an anion detergent that disrupts the tertiary structure of proteins by breaking down the protein-protein disulphide bonds resulting in a linear structured protein. Additionally, SDS coats the protein with a uniform negative charge. This masks the intrinsic charges on the R-groups. The net negative charge surrounded around the protein causes the migration of the protein towards the positive anode. The rate of migration of proteins is dependent on the molecular weight of the protein. Lower molecular weight proteins migrate faster through the pores of the gel than higher molecular weight proteins (Figure 2.11).

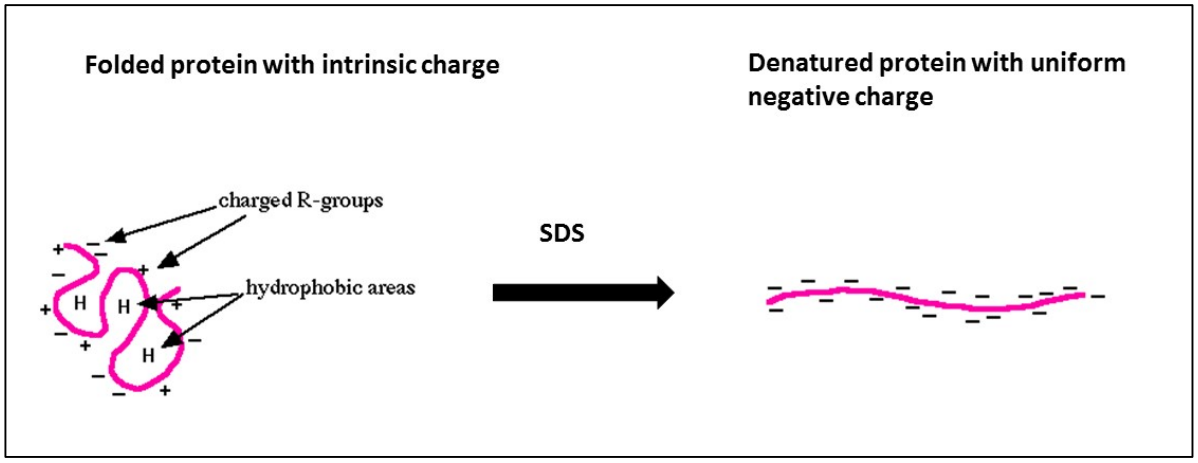

Figure 2.10: Unfolding of proteins coated with SDS. (Prepared by author).

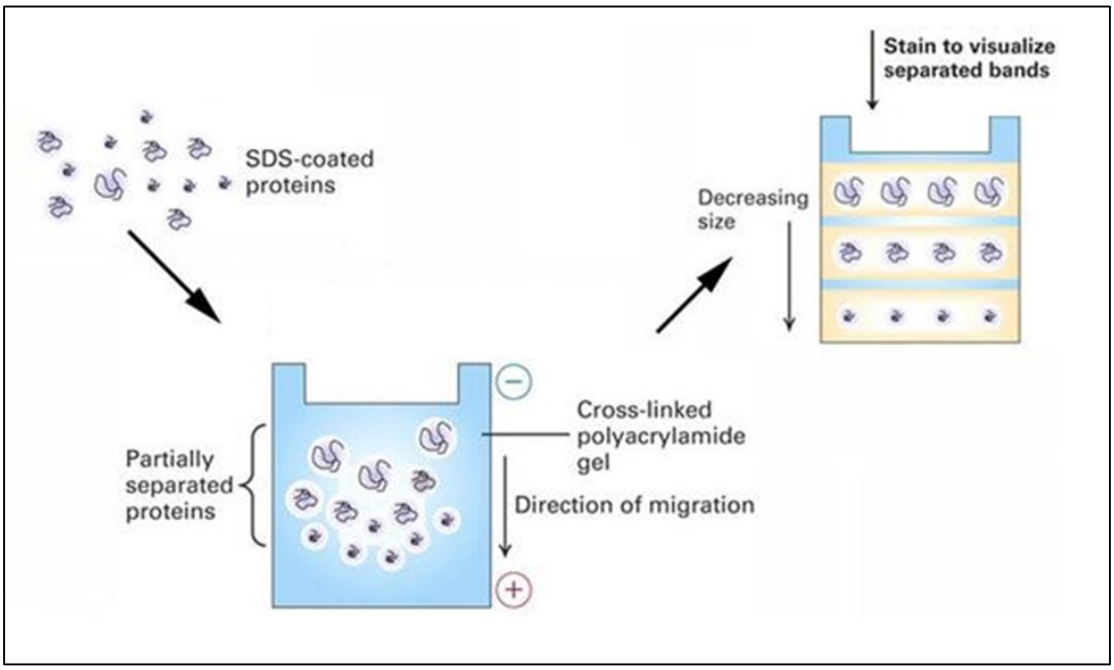

Figure 2.11: Migration of SDS coated proteins along a polyacrylamide gel. (Biochemistry laboratory manual, 2015).

Following protein standardisation, the samples (25 µl- Thp-1; 40 µl-PBMC) were electrophoresed in SDS-PAGE gels (4 % stacking gel, 7.5 % resolving gel) for 1.5 hrs at 150 V (Bio-Rad compact power supply).

2.7.4. Electro-transfer

The electro-transfer procedure is based on the conduction of current from the cathode to the anode. This current is created by the transfer buffer and allows for the transfer of proteins from the gel to the membrane (Figure 2.12).

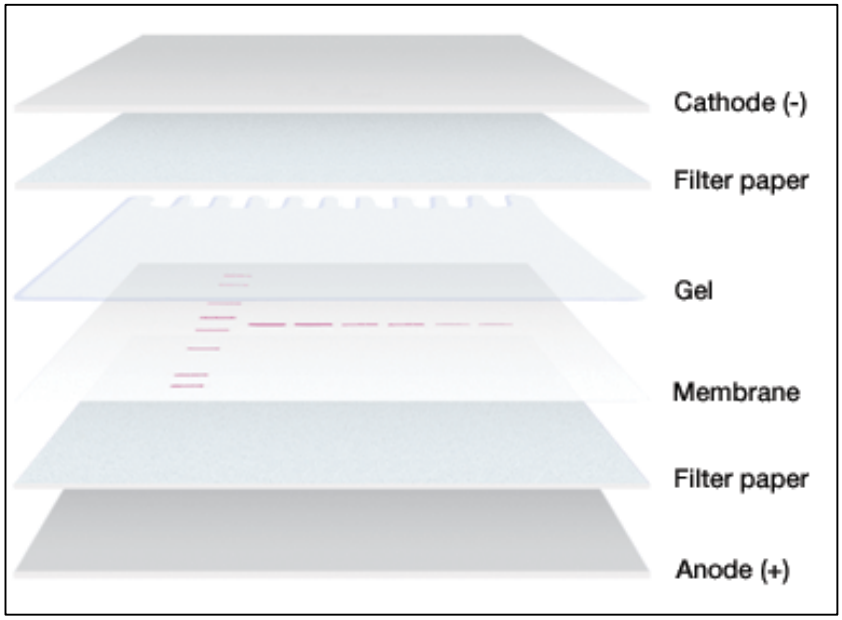

Figure 2.12: Layout used for electro-transfer. (Bio-Rad Laboratories, Inc., 2015).

The separated proteins were electro-transferred onto nitrocellulose membranes for 30 min (400 mA) using the Trans-Blot Turbo Transfer system (Bio-Rad).

2.7.5. Immuno-blotting

In western blotting, it is important to block unbound sites on the membrane to reduce the amount of non-specific binding of proteins. Subsequent to blocking, the membrane is incubated with a primary antibody specific to the target protein. Once the primary antibody binds to target protein, the membrane is washed to remove unbound primary antibody. Thereafter, the membrane is incubated with a secondary antibody conjugated with an enzyme e.g. HRP, that binds to the primary antibody. HRP oxidizes the luminescent substrate, luminol in the presence of H_2O_2 to produce a luminescent light. This light is intensified a 1000-fold increase by enhancers present in the substrate and is detected on a photographic film (Figure 2.13).

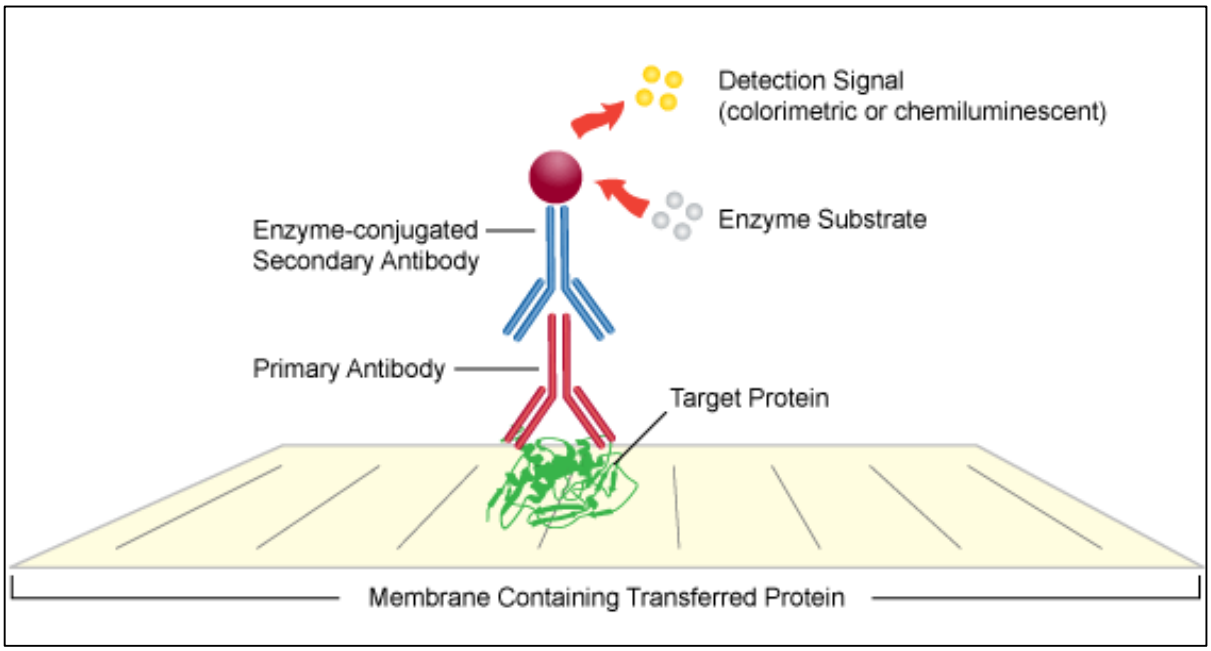

Figure 2.13: Antibody-antigen complex used for the detection of proteins. (Leinco Technologies, Inc., 2015).

Following electro-transfer of proteins, the membranes were blocked for 1 h (RT) with 5% bovine serum albumin (BSA) in Tris Buffer Saline with tween 20 (TTBS- NaCl, KCl, Tris, dH_2O, 0.5% tween 20, pH 7.5) or 5% Non-Fat Dry Milk (NFDM) in TTBS for phospho- and non-phospho-antibodies, respectively. Thereafter, the membranes were incubated with primary antibody [rabbit anti-p-Akt (13038), mouse anti-p-ERK (9106), mouse anti-p-JNK (9255), rabbit anti-p38 (14451), rabbit anti-Bax (5023), rabbit anti-p-Bcl-2 (2827), Cell Signalling, 1: 1000; β-actin (A3854), Sigma Aldrich, 1: 5000] for 1 h (RT) and then overnight at 4^0C. The membranes were washed five times with TTBS (10 min intervals) and incubated (RT) with horseradish peroxidase (HRP)- conjugated secondary antibody [goat anti-rabbit (ab6112), anti-mouse (ab97046), 1: 5000] (1 h- Thp-1 protein expressions; 2 hrs- PBMC protein expressions). Once more, the membranes were washed 5 times with TTBS (10 min intervals). Protein band images were detected using Clarity Western ECL Substrate and captured using Alliance 2.7 Image documentation system (UViTech). The expression of protein bands were analysed using UViBand Advanced Image Analysis software v12.14 (UViTech). The data was expressed as relative band intensity (RBI).

2.8. Statistical analysis

Statistical analyses were performed using GraphPad Prism v5.0 software. GraphPad Prism Software was used for the unpaired t-test with Welch's correction to assess the differences between samples. Level of significance (p) was established at a $p<0.05$.

CHAPTER 3

RESULTS

3.1 Cell viability

3.1.1 WST-1 assay

The WST-1 assay was used to determine the immunotoxicity of FA on healthy PBMCs and Thp-1 cells. At a concentration range of 30-300 µg/ml, FA decreased cell viability in both PBMCs and Thp-1 cells over a 24 h incubation period. An IC_{50} of 240.8 µg/ml (Figure 3.1A) and 107.7 µg/ml (Figure 3.1B) was extrapolated from the dose response curve for PBMCs and Thp-1 cells respectively; and was used in all subsequent assays.

A **B**

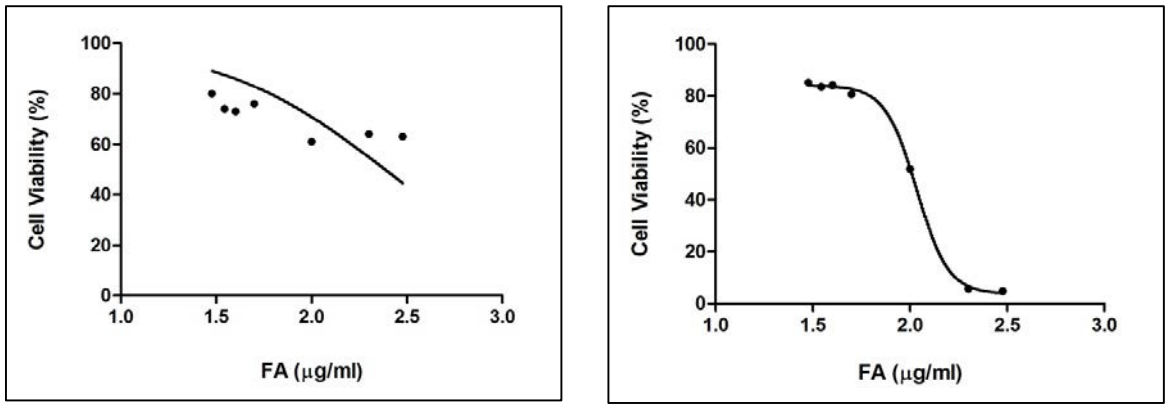

Figure 3.1: Effect of FA on healthy PBMC (A) and Thp-1 (B) cell viability.

3.2 Analysis of cell death parameters

3.2.1 Annexin V-FITC staining

Flow cytometry was performed using Annexin V-FITC and PI staining to determine the mode of cell death induced by FA on PBMCs and Thp-1 cells. FA significantly induced the externalization of phosphatidylserine in PBMCs and Thp-1 cells by 1.42 (18.43 $\pm$ 0.006% vs. 26.16 $\pm$ 0.003%; p=0.0003) and 2.27 (8.03 $\pm$ 0.004% vs.18.19 $\pm$ 0.002%; p<0.0001) fold, respectively (Figure 3.2A and 3.2B).

A **B**

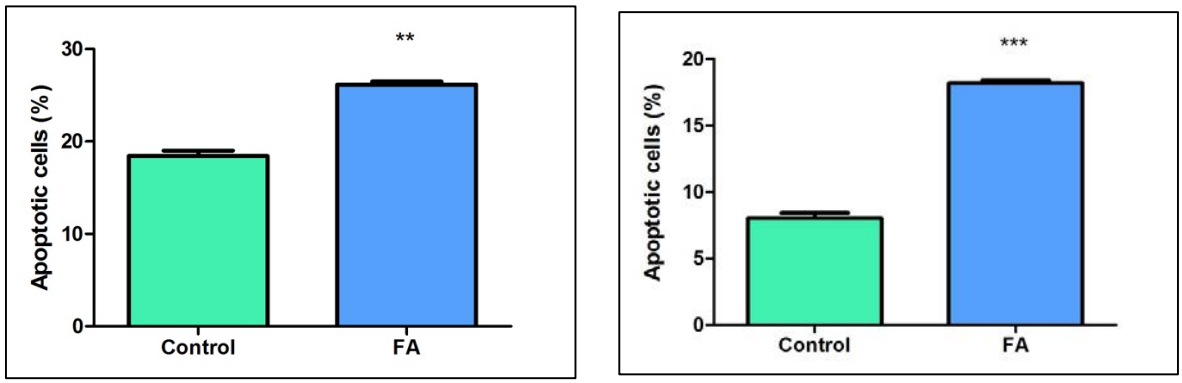

Figure 3.2: Effect of FA on the externalization of phosphatidylserine in healthy PBMCs (A) and Thp-1 cells (B). **p<0.005; ***p<0.0001.

3.2.2 Caspase activity

To confirm the induction of cell death and to elucidate the induced PCD pathway, caspase activities of 8, 9 and 3/7 were measured using luminomnetry. In PBMCs, FA substantially decreased caspase 8 activity by 0.81 fold (1.09 $\pm$ 0.001x10^4 RLU vs. 0.88 $\pm$ 0.042x10^4 RLU; p=0.0022), caspase 9 by 0.73 fold (10.89 $\pm$ 0.609x10^4 RLU vs. 7.92 $\pm$ 0.241x10^4 RLU; p=0.0070) and caspase 3/7 activities by 0.10 fold (1.19 $\pm$ 0.258x10^4 RLU vs. 0.12 $\pm$ 0.026x10^4 RLU; p=0.0035), relative to the control (Table 1). In Thp-1 cells, FA decreased caspase 8 activity by 0.74 fold (4.52 $\pm$ 0.306x10^4 RLU vs. 3.3265 $\pm$ 0.021x10^4 RLU; p=0.0211) and greatly increased caspase 9 activity by 1.43 fold (62.67 $\pm$ 3.701x10^4 RLU vs. 89.37 $\pm$ 0.590x10^4 RLU; p=0.0065) and caspase 3/7 activity by 5.33 fold (0.82 $\pm$ 0.482x10^4 RLU vs. 4.38 $\pm$ 0.604x10^4 RLU; p=0.0041) when compared to the control (Table 2).

Table 1: Effect of FA on caspase (8, 9, 3/7) activity in healthy PBMCs

	Mean ± SD (RLU x10^4)		Fold change	p value
	PBMC			
	Control	FA		
Caspase 8	1.0918 ± 0.0007	0.8831 ± 0.0419	0.81	<0.005**
Caspase 9	10.8855 ± 0.6094	7.9185 ± 0.2409	0.73	<0.05*
Caspase 3/7	1.1858 ± 0.2581	0.1218 ± 0.0261	0.10	<0.005**

SD: standard deviation; **RLU:** relative light units; *p<0.05; **p<0.005.

Table 2: Effect of FA on caspase (8, 9, 3/7) activity in Thp-1 cells

	Mean ± SD (RLU x10^4)		Fold change	p value
	Thp-1			
	Control	FA		
Caspase 8	4.5235 ± 0.3055	3.3265 ± 0.0206	0.74	<0.05*
Caspase 9	62,6683 ± 3.7013	89.3652 ± 0.5900	1.43	<0.05*
Caspase 3/7	0.8210 ± 0.4816	4.3758 ± 0.6041	5.33	<0.005**

SD: standard deviation; **RLU:** relative light units; *p<0.05; **p<0.005.

3.2.3 Tumour necrosis factor-α

To confirm caspase 8 and 3/7 activities, TNF-α levels were measured using ELISA. FA had no significant effect on TNF-α levels in both PBMCs (0.96 fold change; 172.92 ± 6.455 pg/ml vs. 165.42 ± 10.887 pg/ml; p=0.3015) and Thp-1 cells (0.97 fold change; 162.92 ± 8.660 pg/ml vs. 157.92 ± 8.767 pg/ml; p=0.4540) relative to the controls (Figure 3.3A and 3.3B).

A B

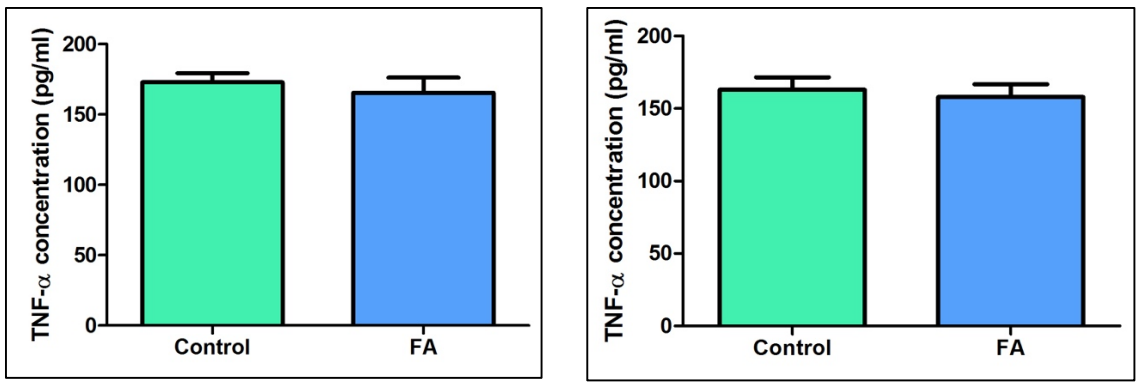

Figure 3.3: TNF-α concentration in healthy PBMCs (A) and Thp-1 cells (B).

3.3 Oxidative stress

3.3.1 Lipid peroxidation

To determine the induction of cell death by a stress response the lipid peroxide, MDA was quantified using the TBARS assay. Lipid peroxidation occurs following an increase in ROS and thus serves as an indicator of oxidative stress. MDA levels were increased by 7.59 and 1.59 fold in PBMCs (0.02 ± 0.010 µM vs. 0.16 ± 0.016 µM; p=0.0006) and Thp-1 treated cells (0.18 ± 0.020 µM vs. 0.28 ± 0.010 µM; p=0.0039) respectively (Figure 3.4A and 3.4B).

A B

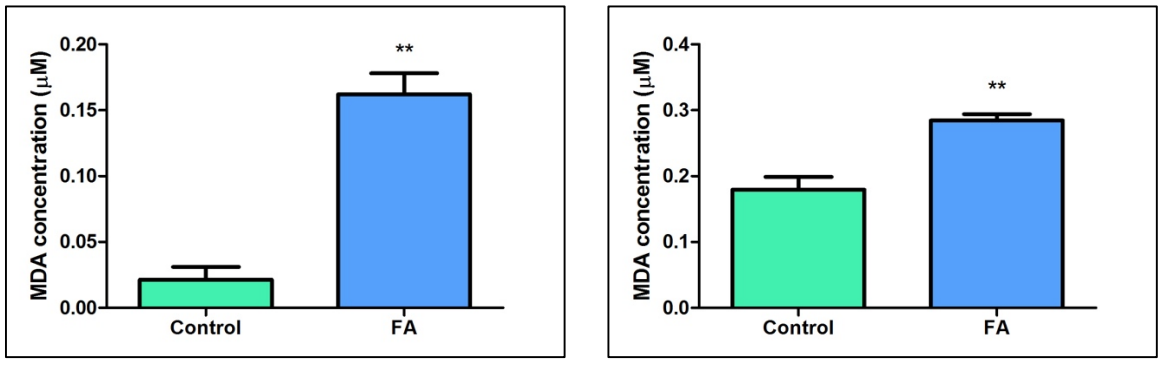

**Figure 3.4: MDA concentration levels (µM) in healthy PBMCs (A) and Thp-1 cells (B) treated with FA. ****p<0.005.

3.3.2 Mitochondrial membrane potential

To confirm the production of ROS, flow cytometric analysis using the JC-1 stain was performed. FA had no effect on the mitochondrial membrane potential in PBMCs (1.04 fold change; 40.97 ± 4.210% vs. 42.64 ± 0.240%; p=0.5643) but significantly increased the mitochondrial membrane potential in Thp-1 cells by 1.95 fold (33.58 ± 1.425% vs. 65.48 ± 0.329%; p=0.0007) when compared to the controls (Figure 3.5A and 3.5B).

A **B**

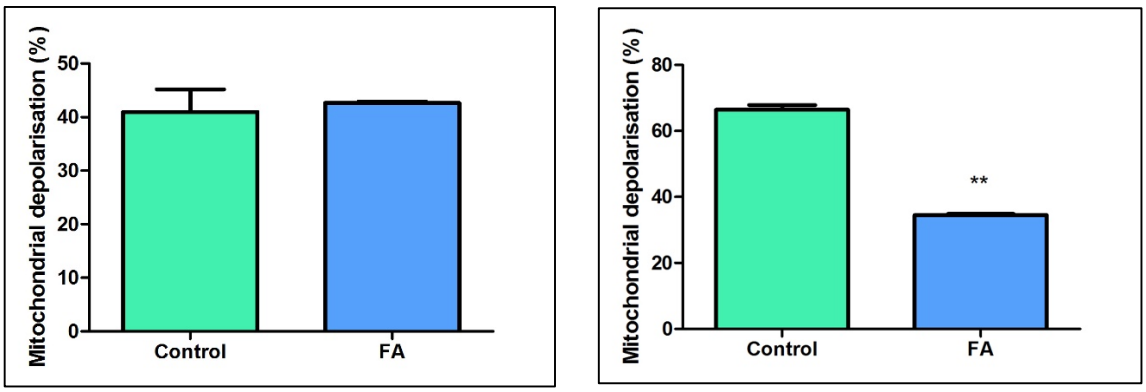

**Figure 3.5: Mitochondrial depolarization in healthy PBMCs (A) and Thp-1 cells (B) treated with FA. ****p<0.005.

3.3.3 ATP levels

To confirm the toxicity of FA on PBMCs and Thp-1 cells, ATP levels were measured using the ATP CellTitre Glo reagent. FA significantly decreased ATP levels in PBMCs by 0.16 fold (38.97 ± 1.183x10^4 RLU vs. 6.11 ± 0.266x10^4 RLU; p=0.0002) and by 0.52 fold in Thp-1 cells (225.21 ± 8.014x10^4 RLU vs. 117.26 ± 10.017x10^4 RLU; p=0.0007) in comparison to the relative controls (Figure 3.6A and 3.6B).

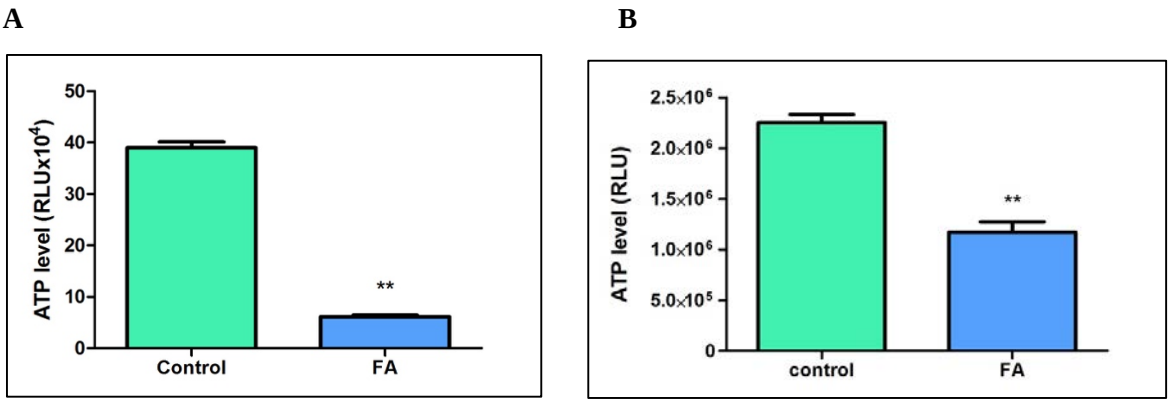

Figure 3.6: ATP levels in healthy PBMCs (A) and Thp-1 cells (B) treated with FA. RLU: Relative light units; **p<0.005.

3.4 Western blotting

To confirm caspase-dependent and –independent cell death, protein expressions of Bax and p-Bcl-2 were determined using western blotting. In PBMCs, FA significantly decreased Bax protein expression by 0.71 fold (0.07 ± 0.007 RBI vs. 0.05 ± 0.005 RBI; p=0.0201) and increased p-Bcl-2 protein expression by 1.81 fold (0.13 ± 0.008 RBI vs. 0.15 ± 0.004 RBI; p=0.0455) when compared to the control (Figure 3.7A and 3.8A). In Thp-1 cells, FA had no effect on the protein expression of Bax (0.98 fold; 0.04 ± 0.002 RBI vs. 0.03 ± 0.001 RBI; p=0.6130) but significantly decreased the protein expression of p-Bcl-2 by 0.78 fold (0.07 ± 0.001 RBI vs. 0.05 ± 0.002 RBI; p=0.0007) when compared to the control (Figure 3.7B and 3.8B).

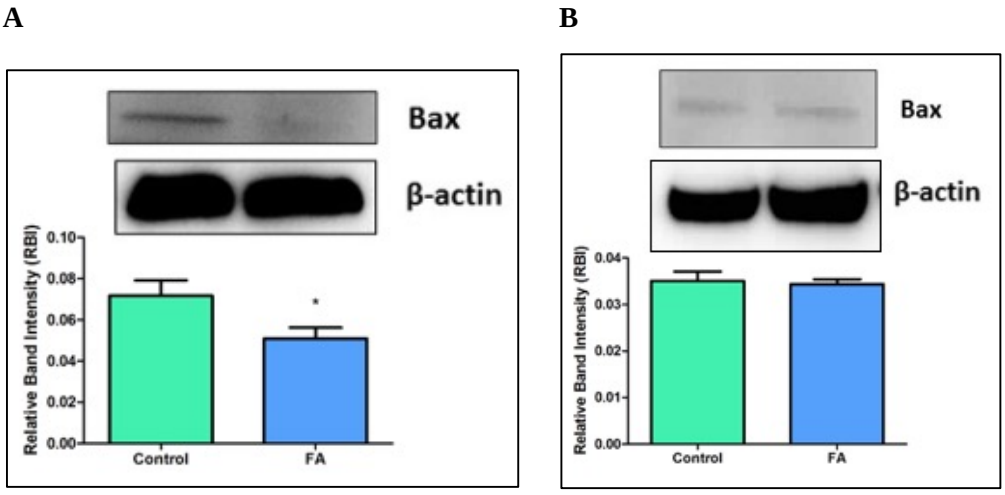

Figure 3.7: Relative band intensities of Bax protein expression in healthy PBMCs (A) and Thp-1 cells (B). *p<0.05.

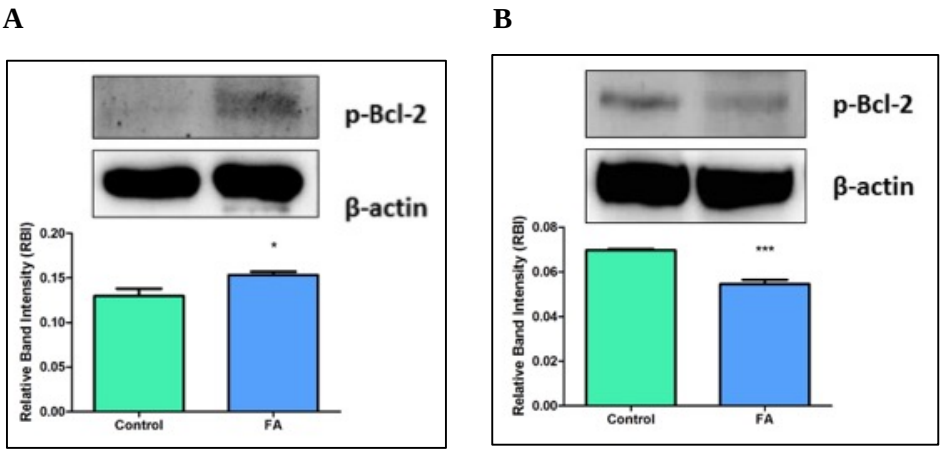

Figure 3.8: Relative band intensities of p-Bcl-2 protein expression in healthy PBMCs (A) and Thp-1 cells (B). *p<0.05.

To determine the molecular events in the immunotoxicity of FA, the involvement of MAPK and p-Akt protein expressions using western blotting was investigated.

In PBMCs, FA had no significant effect on p-Akt protein expression (1.08 fold; 0.19 ± 0.005 vs. 0.21 ± 0.016 RBI; p=0.1640) (Figure 3.9A). However, FA significantly increased p-Akt protein expression by 1.76 fold (0.03 ± 0.001 vs. 0.06 ± 0.014; p=0.0412) in Thp-1 cells (Figure 3.9B).

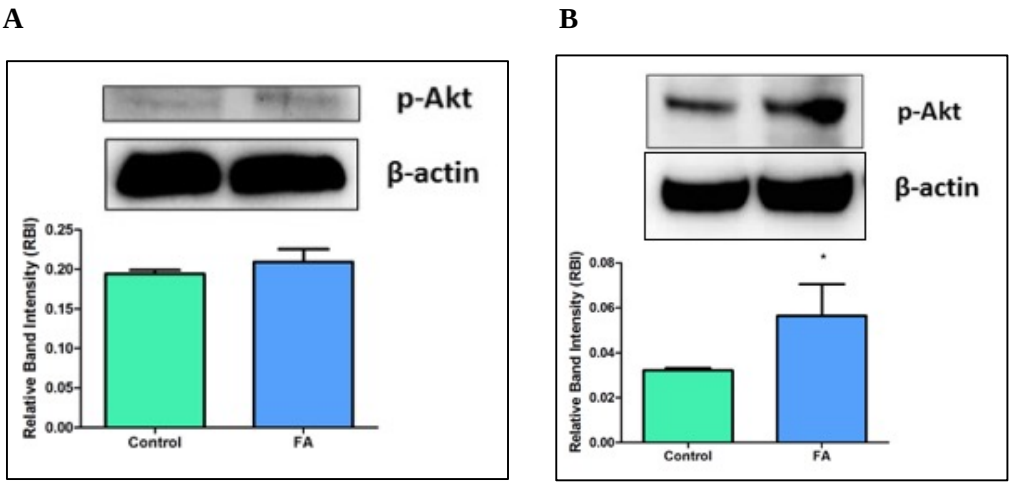

Figure 3.9: Relative band intensities of p-Akt protein expression in healthy PBMCs (A) and Thp-1 cells (B). *p<0.05.

Protein expression of p-ERK 42 kDa fragment and 44 kDa fragment were significantly increased by FA by 1.94 (0.09 ± 0.005 RBI vs. 0.18 ± 0.025 RBI; p=0.0271) and 1.38 (0.08 ± 0.001 RBI vs. 0.10 ±

0.004 RBI; p=0.0006) fold in PBMCs, respectively (Figure 3.10A). In Thp-1 cells, FA significantly increased p-ERK 42 kDa and 44 kDa fragments by 1.56 (0.04 ± 0.001 RBI vs. 0.60 ± 0.001 RBI; p<0.0001) and 2.04 (0.22 ± 0.017 RBI vs. 0.45 ± 0.030 RBI; p=0.0002) fold, respectively (Figure 3.10B).

A

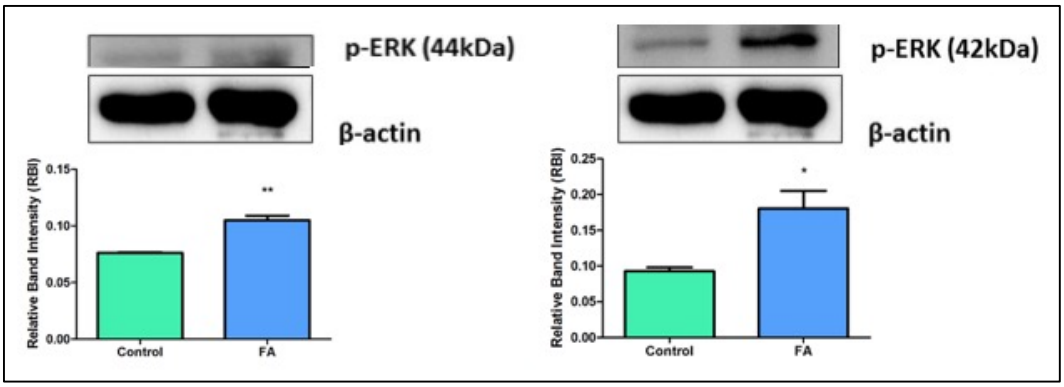

B

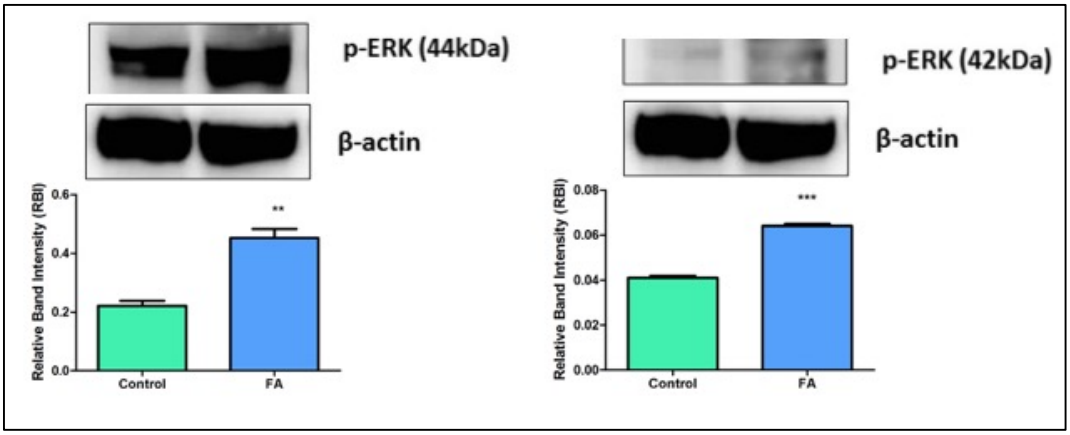

Figure 3.10: Relative band intensities of p-ERK protein expression in healthy PBMCs (A) and Thp-1 cells (B). *p<0.05; **p<0.005; ***p<0.0001.

Protein expression of p-JNK 46 kDa fragment and 54 kDa fragment were significantly increased by FA by 1.42 fold (0.05 ± 0.005 RBI vs. 0.07 ± 0.0004 RBI; p=0.0035) and 1.08 (0.06 ± 0.008 RBI vs. 0.07 ± 0.002 RBI; p=0.0454) fold in PBMCs, respectively (Figure 3.11A). In Thp-1 cells, FA significantly decreased p-JNK 46 kDa and 54 kDa fragments by 0.70 (0.28 ± 0.071 RBI vs. 0.26 ± 0.021 RBI; p=0.0461) and 0.91 (0.28 ± 0.006 RBI vs. 0.20 ± 0.012 RBI; p=0.0055) fold, respectively (Figure 3.11B).

A

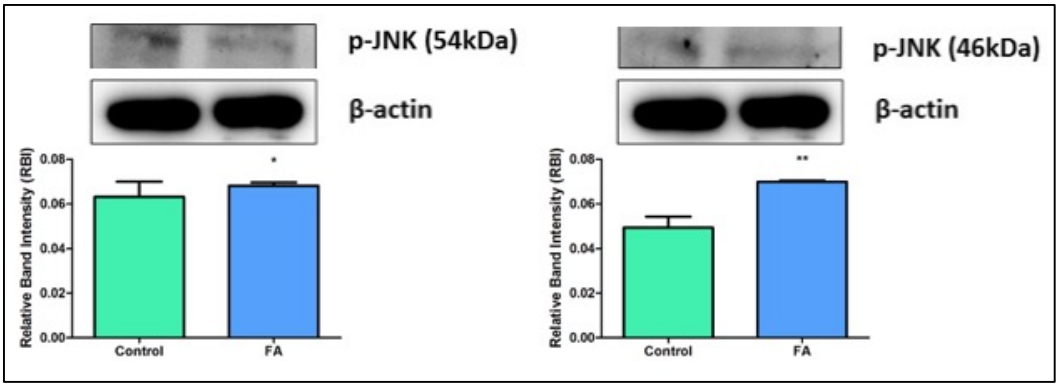

B

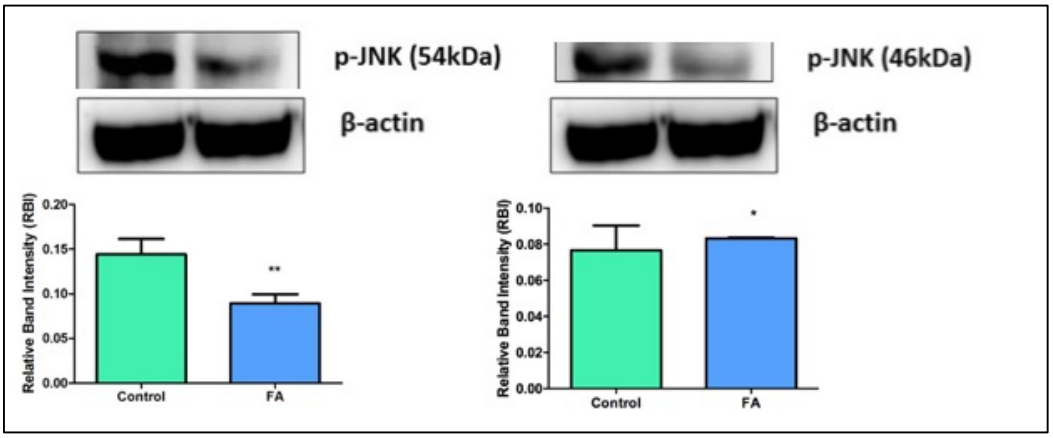

**Figure 3.11: Relative band intensities of p-JNK protein expression in healthy PBMCs (A) and Thp-1 cells (B). ***p<0.05; **p<0.005.

Furthermore, FA significantly increased the protein expression of p38 in PBMCs by 1.16 fold (0.43 ± 0.011 RBI vs. 0.50 ± 0.034 RBI; p=0.0428) and had no significant effect on p38 protein expression in Thp-1 cells (0.62 fold; 0.50 ± 0.027 RBI vs. 0.49 ± 0.019 RBI; p=0.8446) (Figure 3.12A and 3.12B respectively)

A **B**

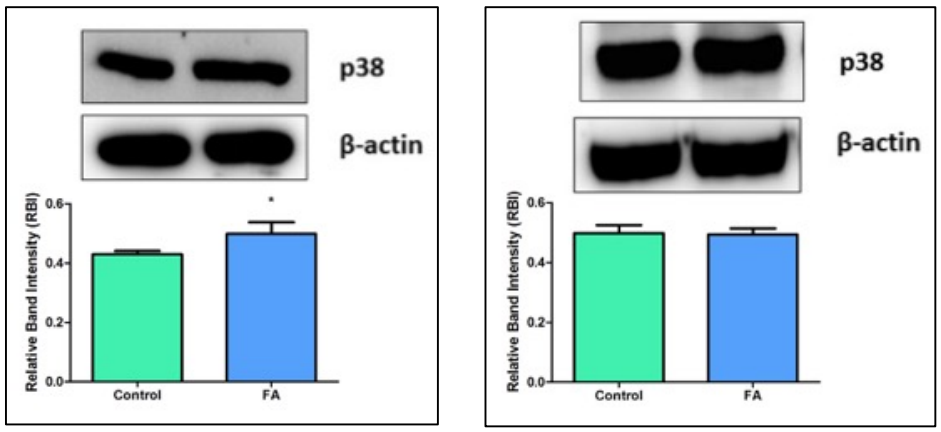

Figure 3.12: Relative band intensities of p38 protein expression in healthy PBMCs (A) and Thp-1 cells (B). *$p<0.05$.

CHAPTER 4

DISCUSSION

FA is potent divalent ion chelator with high toxicity to plants and animals (Bochner *et al.,* 1980). To date, no study has investigated the molecular toxicity of FA on human models and its effect on the immune system. Thus, in this study, we assessed the immunotoxicity of FA on healthy PBMCs and Thp-1 cells, and its effects on the expression of MAPKs and Akt.

This study showed that FA was immunotoxic to both PBMCs and Thp-1 cells as evidenced by their decreased cell viabilities (WST-1 assay) (Figure 3.1A and 3.1B). FA immunotoxicity (increased apoptosis) on PBMCs and Thp-1 cells was assessed using flow cytometry. Phosphatidylserine, a phospholipid present on the inner (cytosolic) plasma membrane, becomes exposed on the outer plasma membrane upon induction of PCD (Zitvogel *et al.,* 2010). The results showed that FA significantly increased the externalization of phosphatidylserine in both PBMCs and Thp-1 cells by 26.16% and 18.19%, respectively (Figure 3.2A and 3.2B). This result is consistent with the decreased cell viability (WST-1 assay) triggered by exposure to FA.

Given that the externalization of phosphatidylserine occurs during apoptotic and paraptotic cell death, activities of caspases 8, 9 and 3/7 were assessed using luminometry to determine the type of PCD induced by FA in PBMCs and Thp-1 cells (apoptosis requires caspase activation and paraptosis is independent of caspase activity). In Thp-1 cells, caspase 8 activity was decreased, while caspase 9 and 3/7 activities were significantly increased (Table 2). This result suggests that FA induced intrinsic apoptosis in Thp-1 cells as no change in TNF-α levels were observed when compared to the control (Figure 3.3B). Unchanged TNF-α levels prevent activation of caspase 8 and thus, the extrinsic apoptotic pathway. In PBMCs treated with FA, a substantial decrease in caspase 8, 9 and 3/7 activities were observed (Table 1). This suggests that FA induced paraptosis in PBMCs as evidenced by the externalization of phosphatidylserine independent of caspase activation. Additionally, TNF-α levels in PBMCs remained unchanged following treatment with FA (Figure 3.3A). This again, may prevent the activation of caspase 8 and subsequent extrinsic cell death.

To confirm caspase-dependent and –independent cell death, protein expressions of the pro-apoptotic protein Bax and anti-apoptotic protein p-Bcl-2 were determined using western blotting. Bcl-2 family

proteins are central in regulating the mitochondrial apoptotic death pathway (Hemmati *et al*., 2002). Bcl-2 prevents apoptosis by forming a complex with pro-apoptotic proteins such as Bax, thereby inhibiting the function of Bax (Hemmati *et al.,* 2002; Wan *et al.,* 2008). Phosphorylation of Bcl-2 compromises its protein stability and affects its ability to dimerize with pro-apoptotic proteins (Huang and Cidlowski, 2002). Thus, dissociation from the complex at the mitochondrial membrane leads to the formation of mPTP and subsequent caspase activation (Zhou *et al*., 2011). In agreement with the increased caspase 9 and 3/7 activities in Thp-1 cells, FA notably decreased p-Bcl-2 expression resulting in apoptotic cell death (Figure 3.8B). However, FA had no significant effect on the expression of Bax in Thp-1 cells (Figure 3.7B). This may be due to the deletion of the p53 gene in the Thp-1 cell line; p53 acts as a transcription factor for Bax expression and recruitment to the mitochondrial membrane. In PBMCs, FA increased p-Bcl-2 expression (Figure 3.8A) and decreased Bax expression (Figure 3.7A), corresponding with the decreased caspase 8, 9 and 3/7 activities. An increase in p-Bcl-2 expression will maintain the mitochondrial membrane integrity and subsequent mitochondrial membrane potential by preventing the release of cytochrome c, activation of caspase 9 and the initiation of intrinsic apoptosis, further validating the induction of paraptosis in PBMCs by FA.

The free radicals, generated during oxidative phosphorylation causes oxidative damage to proteins, DNA and phospholipids (Son *et al.,* 2011). Oxidative degradation of lipids results in the formation of lipid peroxides such as MDA and 4-hydroxynonenal (HNE) (Barrera, 2012). The TBARS assay measures levels of MDA and is a good indicator of oxidative stress. There was a substantial increase of MDA levels in both PBMCs and Thp-1 cells treated with FA (Figure 3.4A and 3.4B), indicative of increased oxidative stress. To further confirm FA-induced oxidative stress, flow cytometric analysis of mitochondrial membrane potential showed that mitochondrial depolarisation was notably increased in Thp-1 cells (Figure 3.5B). This could be due to the weak acidic nature of FA as weak acids act as proton carriers across lipid membranes disrupting the proton gradient along the ETC. Additionally, ROS targets the mPTP resulting in the release of cytochrome c and the subsequent activation of the intrinsic apoptotic program (Marchi *et al*., 2011), correlating with the results obtained for Thp-1 cells. However, in PBMCs, FA had no significant effect on the mitochondrial membrane potential (Figure 3.5B); this may be due to the decreased expression of the pro-apoptotic protein Bax and the increased expression of the anti-apoptotic protein Bcl-2 as a decreased Bax expression promotes the anti-apoptotic activity of Bcl-2 thereby maintaining mitochondrial membrane potential.

To confirm FA depletion of energy levels in PBMCs and Thp-1 cells, ATP levels were measured

using luminometry. Reducing equivalents generated by the Kreb's cycle are channeled through the ETC creating a proton gradient by pumping protons across the mitochondrial membrane space (Harper *et al.,* 2004). The resultant proton-motive force directs the activity of ATP synthase and hence ATP levels (Harper *et al.,* 2004). The ATP levels in both PBMCs and Thp-1 cells were significantly decreased by FA treatment (Figure 3.6A and 3.6B) and this is substantiated by the decreased cell viability and increased mitochondrial membrane depolarisation in Thp-1 cells. Additionally, the activation of ATP dependent caspases -9 and -3/7 may further explain the reduction of ATP levels. However, in PBMCs, the decreased ATP level may be attributed to ATP dependent protein kinases.

Intracellular ROS not only alters cellular integrity but is also important to MAPK and Akt signaling cascades (Kim *et al.,* 2014). Studies suggest that prolonged activation of MAPK and Akt signaling may induce cell death and that ROS acts as a second messenger in the activation of MAPK and Akt signaling pathways (Son *et al.,* 2011). FA increased ROS generation and up-regulated protein expressions of ERK and Akt in Thp-1 cells when compared to the control (Figure 3.10B and 3.9B). Although ERK and Akt signaling pathways are well known for their role in promoting cell survival, recent studies demonstrated their ability in potentiating apoptosis (Park, 2014). Prolonged activation of ERK may be due to the inhibition of tyrosine phosphatases (Harper *et al*., 2004). Tyrosine phosphatases are a group of enzymes responsible for the removal of phosphate groups on phosphorylated tyrosine residues, hence inactivating the protein (Harper *et al*., 2004). However, these enzymes are sensitive to ROS and become oxidized, thereby inhibiting its activity and prolonging ERK activation (Harper *et al*., 2004). Additionally, ERK activity up-regulates the pro-apoptotic protein Bax (Harper *et al.,* 2004). Accordingly, increased ERK activity corresponds with increased Bax expression, activation of caspase 9 and 3/7 and the induction of cell death in Thp-1 treated cells. Furthermore, a study by Nogueira *et al.,* (2008) showed that Akt activation had sensitized cells to ROS-induced apoptosis by increasing levels of intracellular ROS via increased oxygen consumption and the inhibition of ROS scavengers. Moreover, sustained Akt activation leads to the inhibition of FOXO transcription factors, which are associated with the up-regulation of anti-oxidant protein expressions (Los *et al*., 2009). An impaired anti-oxidant system, increases the cells susceptibility to oxidative damage and cell death. Therefore, increased Akt activity correlates with the induction of lipid peroxidation and cell death in Thp-1 cells.

JNK and p38 MAPK signaling pathways are generally directed towards initiating cell death upon activation by stress signals. Recently, however, these signaling pathways have been associated in both

cell death and survival signaling (Zhang and Liu, 2002). FA significantly decreased JNK activation and had no effect of p38 protein expression (Figure 3.11B and 3.12B). A study by Pedram and colleagues (1998) documented the cross-talk between the ERK and JNK MAPKs. These authors reported the activation of JNK by ERK MAPK, following the activation of ERK by vascular endothelial growth factor (VEGF). In turn, JNK had stimulated ERKs proliferative signaling. Thus, a decrease in JNK activity hinders the cross-talk between JNK and ERK MAPKs, preventing survival signaling by ERK. Additionally, JNK signaling regulates the expression of Bcl-2 and is up-regulated in response to JNK activation. This substantiates the activation of ERK death signaling, the decrease in p-Bcl-2 expression and the induction of cell death in Thp-1 cells exposed to FA.

Although the molecular activation of paraptosis is unknown, studies have suggested the involvement of MAPK signaling in the induction of cell death. In PBMCs, FA greatly increased the expression of ERK, JNK and p38 MAPKs, and slightly increased Akt activity (Figure 3.9A, 3.10A, 3.11A and 3.12A). However, Akt activation was not significant. Sperandio *et al.,* (2000) reported the participation of ERK and JNK activity in mediating paraptosis stimulated by IGFIR, and that inhibition of these MAPKs prevented the induction of paraptosis in 293T cells. Another study by Yumnam *et al.,* (2014) showed the involvement of ERK MAPK in hesperidin-induced paraptosis of human hepatocellular carcinoma (HepG2) cells. Sugimori and colleagues (2015) also reported the activation of JNK in paraptosis induction in HL-60 and NB4 human promyelocytic leukaemic cell lines and in bone marrow blasts treated with benfotiamine. Contrary to Sperandio *et al.,* (2000) and Yumnam *et al.,* (2014) benfotiamine had inhibited the activity of ERK in bone marrow blasts and had no effect on ERK activity in HL-60 and NB4 cell lines. This suggests that the involvement of MAPK in the induction of paraptosis may be dependent on the cell type and type of activation. Additionally, caspase 9 had been reported to be a direct target of ERK MAPK, and that phosphorylation at threonine 125 on caspase 9 inhibits its pro-apoptotic activity (Sperandio *et al*., 2000). These findings support the activation of MAPK signaling pathways in the induction of paraptosis in PBMCs treated with FA.

CHAPTER 5

CONCLUSION

The toxicity of FA has been documented in several plant and animal species. In contrast, recent preliminary studies, show the potential of FA as an anti-viral agent due to its ability to chelate divalent ions. This highlights the importance in determining the toxicity of FA before employing it as a therapeutic agent. Therefore, this study was conducted to determine the immunotoxic potential of FA on normal healthy PBMCs and Thp-1 cells.

FA was immunotoxic to both healthy human PBMCs and Thp-1 cells. FA induced paraptosis in PBMCs mediated by MAPK activity. In Thp-1 cells, FA initiated intrinsic apoptosis as evidenced by an impaired mitochondrial function and activation of caspases 9 and 3/7; and the up-regulation of Akt and ERK activity suggesting their involvement in the immunotoxicity of FA in Thp-1 cells.

While this study shows the immunotoxicity of FA in both normal PBMCs and Thp-1 cells, it should be noted that the concentration used to induce toxicity in Thp-1 cells was significantly less than that of PBMCs, suggesting that Thp-1 cells are more susceptible to FA toxicity than PBMCs. The Thp-1 cell line is a cancerous cell line and suggests the potential of FA as a therapeutic agent.

Further research on the toxicity of FA on other cell lines and its potency during a chronic treatment are required. In addition, the immunotoxicity of FA on an *in vivo* model presents future research opportunities.

REFERENCES

3D Biomatrix (2015) *Are the cells in my spheroids living and growing or are they dying*? [On-line], https://3dbiomatrix.com/cells-spheroids-living-growing-dying/ Accessed 24 November 2015.

Adati, N., Huang, M.C., Suzuki, T., Suzuki, H. and Kojima, T. (2009) High-resolution analysis of aberrant regions in autosomal chromosomes in human leukemia THP-1 cell line. *BMC research notes* **2**(1): 153.

Amin, A.A., Douglas, M.G. and Fernandez-Pol, J.A. (2001) Pharmacological agent comprising picolinic acid, fusaric acid and derivatives thereof. Google patent WO 2001060349 A2.

Auffray, C., Sieweke, M.H. and Geissmann, F. (2009) Blood monocytes: development, heterogeneity, and relationship with dendritic cells. *Annual review of immunology* **27**: 669-692.

Bacon, C.W., Porter, J.K., Norred, W.P. and Leslie, J.F. (1996) Production of fusaric acid by Fusarium species. *Applied and Environmental Microbiology* **62**(11): 4039-4043.

Barrera, G. (2012) Oxidative stress and lipid peroxidation products in cancer progression and therapy. *ISRN oncology*.

Biochemistry Laboratory Manual (2015) *Determining the Molecular Weight of Lysozyme-Background* [On-line], http://www.chem.fsu.edu/chemlab/bch4053l/character/mwdetermination/background.html Accessed 4 December 2015.

Bio-Rad Laboratories, Inc. (2015) *Protein Blotting Methods* [On-line], http://www.bio-rad.com/en-za/applications-technologies/protein-blotting-methods Accessed 4 December 2015.

Biosciences, B.D. (2011) *Detection of Apoptosis Using the BD Annexin V FITC Assay on the BD FACSVerse™ System* [On-line], https://www.bdbiosciences.com/documents/BD_FACSVerse_Apoptosis_Detection_AppNote.pdf Accessed 4 December 2015.

BioTek Instruments Inc. (2015) *Fluorescent Detection of Drug-Induced Mitochondrial Toxicity* [On-line], http://www.biotek.com/resources/articles/fluorescent-detection-drug-induced-mitochondrial-toxicity.html Accessed 5 December 2015.

Bharathiraja, B., Jayakumar, M., Ramaprabu, C. and Jayamuthunagai, J. (2010) Production Of Fusaric Acid From Cassava Using Fusarium oxysporum MTCC 1755. *Production of Fusaric Acid From Cassava using Fusarium oxysporum MTCC 1755* **9**(10): 26-31.

Bochner, B.R., Huang, H.C., Schieven, G.L. and Ames, B.N. (1980) Positive selection for loss of tetracycline resistance. *Journal of bacteriology* **143**(2): 926-933.

Boldt, S., Weidle, U.H. and Kolch, W. (2002) The role of MAPK pathways in the action of chemotherapeutic drugs. *Carcinogenesis* **23**(11): 1831-1838.

Cuenda, A. and Rousseau, S. (2007) p38 MAP-kinases pathway regulation, function and role in human diseases. *Biochimica et Biophysica Acta (BBA)-Molecular Cell Research* **1773**(8): 1358-1375.

D'Alton, A. and Etherton, B. (1984) Effects of fusaric acid on tomato root hair membrane potentials and ATP levels. *Plant Physiology* **74**(1): 39-42.

Dawn, M. (2012) The Balance between Life and Death: Defining a Role for Apoptosis in Aging. *Journal of Clinical & Experimental Pathology* **4**: 1-10.

Dayem, A.A., Choi, H.Y., Kim, J.H. and Cho, S.G. (2010) Role of oxidative stress in stem, cancer, and cancer stem cells. *Cancers* **2**(2): 859-884.

Dhillon, A.S., Hagan, S., Rath, O. and Kolch, W. (2007) MAP kinase signalling pathways in cancer. *Oncogene* **26**(22): 3279-3290.

Diniz, S.P.S.S. and Oliveira, R.C. (2009) Effects of fusaric acid on Zea mays L. seedlings. *Phyton (Buenos Aires)* 155.

Dragich, M. and Nelson, S. (2014) Gibberella and Fusarium ear rots of maize in Hawai'i. *Plant Disease.*

Eimon, P.M., Kratz, E., Varfolomeev, E., Hymowitz, S.G., Stern, H., Zha, J. and Ashkenazi, A. (2006) Delineation of the cell-extrinsic apoptosis pathway in the zebrafish. *Cell Death & Differentiation* **13**(10): 1619-1630.

Elmore, S. (2007) Apoptosis: a review of programmed cell death. *Toxicologic pathology* **35**(4): 495-516.

Fernandez-Pol, J.A. (1998) Antiviral agent. Google patent US 5767135 A.

Gururajan, M., Chui, R., Karuppannan, A.K., Ke, J., Jennings, C.D. and Bondada, S. (2005) c-Jun N-terminal kinase (JNK) is required for survival and proliferation of B-lymphoma cells. *Blood* **106**(4): 1382-1391.

Gutterman, D.D. (2005) Mitochondria and reactive oxygen species an evolution in function. *Circulation research* **97**(4): 302-304.

Harper, M.E., Bevilacqua, L., Hagopian, K., Weindruch, R. and Ramsey, J.J. (2004) Ageing, oxidative stress, and mitochondrial uncoupling. *Acta physiologica Scandinavica* **182**(4): 321-331.

Hemmati, P.G., Gillissen, B., von Haefen, C., Wendt, J., Starck, L., Guner, D., Dorken, B. and Daniel, P.T. (2002) Adenovirus-mediated overexpression of p14^ A^ R^ F induces p53 and Bax-independent apoptosis. *Oncogene* **21**(20): 3149-3161.

Holmström, K. M. and Finkel, T. (2014) Cellular mechanisms and physiological consequences of redox-depenedent signalling. *Nature Reviews Molecular Cell Biology* **15**(6): 411-421.

Huang, S.T.J. and Cidlowski, J.A. (2002) Phosphorylation status modulates Bcl-2 function during glucocorticoid-induced apoptosis in T lymphocytes. *The FASEB journal* **16**(8): 825-832.

Kaushik, S., Pandav, S.S and Ram, J. (2003) Neuroprotection in glaucoma. *Journal of postgraduate medicine* **49**(1): 90.

Kim, D., Park, G.B. and Hur, D.Y. (2014) Apoptotic signaling through reactive oxygen species in cancer cells. *World J Immunol* **4**(3): 158-173.

Kondoh, K., Torii, S. and Nishida, E. (2005) Control of MAP kinase signaling to the nucleus. *Chromosoma* **114**(2): 86-91.

Kuznetsov, A.V., Margreiter, R., Amberger, A., Saks, V. and Grimm, M. (2011) Changes in mitochondrial redox state, membrane potential and calcium precede mitochondrial dysfunction in

doxorubicin-induced cell death. *Biochimica et Biophysica Acta (BBA)-Molecular Cell Research* **1813**(6): 1144-1152.

Kwiatkowski, M., Sund, C., Ylikoski, J. Mukkala, V.M. and Hemmilä, I. (1989) Metal-chelating 2,6-disubstituted pyridine compounds and their use. Google patent EP 0298939 A1.

Leinco Technologies, Inc. (2015) *General Western Blot Protocol* [On-line], http://www.leinco.com/general_wb Accessed 5 December 2015.

Liu, D., Martino, G., Thangaraju, M., Sharma, M., Halwani, F., Shen, S.H., Patel, Y.C. and Srikant, C.B. (2000) Caspase-8-mediated intracellular acidification precedes mitochondrial dysfunction in somatostatin-induced apoptosis. *Journal of Biological Chemistry* **275**(13): 9244-9250.

Los, M., Maddika, S., Erb, B. and Schulze-Osthoff, K. (2009) Switching Akt: from survival signaling to deadly response. *Bioessays* **31**(5): 492-495.

Marchi, S., Giorgi, C., Suski, J.M., Agnoletto, C., Bononi, A., Bonora, M., De Marchi, E., Missiroli, S., Patergnani, S., Poletti, F. and Rimessi, A. (2011) Mitochondria-ros crosstalk in the control of cell death and aging. *Journal of signal transduction* 2012.

Martelli, A.M., Tabellini, G., Bressanin, D., Ognibene, A., Goto, K., Cocco, L. and Evangelisti, C. (2012) The emerging multiple roles of nuclear Akt. *Biochimica et Biophysica Acta (BBA)-Molecular Cell Research* **1823**(12): 2168-2178.

Mendoza, M.C., Er, E.E. and Blenis, J. (2011) The Ras-ERK and PI3K-mTOR pathways: cross-talk and compensation. *Trends in biochemical sciences* **36**(6): 320-328.

Mertlikova-Kaiserova, H., Nejedla, M., HOLÝ, A. and Votruba, I. (2012) Involvement of MAP Kinases in the Cytotoxicity of Acyclic Nucleoside Phosphonates. *Anticancer research* **32**(2): 497-501.

Microamaze (2015) *Bicinchoninic acid (BCA) assay for proteins* [On-line], http://microamaze.blogspot.co.za/2015/10/bicinchoninic-acid-bca-assay-for.html Accessed 6 December 2015.

Morrison, D. K. (2012) MAP kinase pathways. *Cold Spring Harbor perspectives in biology* **4**(11): a011254.

Murphy, P.A., Hendrich, S., Landgren, C. and Bryant, C.M. (2006) Food mycotoxins: an update. *Journal of food science* **71**(5): R51-R65.

Nogueira, V., Park, Y., Chen, C.C., Xu, P.Z., Chen, M.L., Tonic, I., Unterman, T. and Hay, N. (2008) Akt determines replicative senescence and oxidative or oncogenic premature senescence and sensitizes cells to oxidative apoptosis. *Cancer cell* **14**(6): 458-470.

Park, J.I. (2014) Growth arrest signaling of the Raf/MEK/ERK pathway in cancer. *Frontiers in biology* **9**(2): 95-103.

Pavlovkin, J., Mistrik, I. and Prokop, M. (2004) Some aspects of the phytotoxic action of fusaric acid on primary Ricinus roots. *Plant Soil and Environment* **50**(9): 397-401.

Pearce, E.L. and Pearce, E.J. (2013) Metabolic pathways in immune cell activation and quiescence. *Immunity* **38**(4): 633-643.

Pedram, A., Razandi, M. and Levin, E.R. (1998) Extracellular signal-regulated protein kinase/Jun kinase cross-talk underlies vascular endothelial cell growth factor-induced endothelial cell proliferation. *Journal of Biological Chemistry* **273**(41): 26722-26728.

Promega Corporation (2015) *CellTiter-Glo® 2.0: A Luminescent Cell Viability Assay for Fast, Easy, Everyday Use* [On-line], https://www.promega.com/products/cell-health-and-metabolism/cell-viability-assays/ready-to-use-viability-reagent/ Accessed 5 December 2015.

R&D Systems, Inc. (2015) *R&D Systems® ELISAs: Quality Manufacturing and Evaluation of Performance* [On-line], https://www.rndsystems.com/products/elisas-quality-manufacturing-and-evaluation-performance Accessed 6 December 2015.

Roux, P.P. and Blenis, J. (2004) ERK and p38 MAPK-activated protein kinases: a family of protein kinases with diverse biological functions. *Microbiology and molecular biology reviews* **68**(2): 320-344.

Sanguine Biosciences, Inc. (2013) *Types of immune cells present in human PBMC* [On-line], http://technical.sanguinebio.com/types-of-immune-cells-present-in-human-pbmc/ Accessed 22 May 2015.

Smith, T. (1992) Recent advances in the understanding of Fusarium trichothecene mycotoxicoses. *Journal of animal science* **70**(12): 3989-3993.

Sochr, J., Cinkova, K. and Svorc, L. (2014) Degradation Markers in Nutritional Products a Review. *Austin J Anal Pharm Chem* **1**(1): 1005.

Son, Y., Cheong, Y.K., Kim, N.H., Chung, H.T., Kang, D.G. and Pae, H.O. (2011) Mitogen-activated protein kinases and reactive oxygen species: how can ROS activate MAPK pathways? *Journal of signal transduction* 2011.

Sperandio, S., de Belle, I. and Bredesen, D.E. (2000) An alternative, nonapoptotic form of programmed cell death. *Proceedings of the National Academy of Sciences* **97**(26): 14376-14381.

Sperandio, S., Poksay, K., De Belle, I., Lafuente, M.J., Liu, B., Nasir, J. and Bredesen, D.E. (2004) Paraptosis: mediation by MAP kinases and inhibition by AIP-1/Alix. *Cell Death & Differentiation* **11**(10): 1066-1075.

Sugimori, N., Espinoza, J.L., Trung, L.Q., Takami, A., Kondo, Y., An, D.T., Sasaki, M., Wakayama, T. and Nakao, S. (2015) Paraptosis Cell Death Induction by the Thiamine Analog Benfotiamine in Leukemia Cells. *PloS one* **10**(4): e0120709.

Terasawa, F. and Kameyama, M. (1971) The clinical trial of a new hypotensive agent, fusaric acid (5-butylpicolinic acid): The preliminary report. *Japanese circulation journal* **35**(3): 339-357.

Wan, K.F., Chan, S.L., Sukumaran, S.K., Lee, M.C. and Victor, C.Y. (2008) Chelerythrine induces apoptosis through a Bax/Bak-independent mitochondrial mechanism. *Journal of Biological Chemistry* **283**(13): 8423-8433.

Wang, H. and Ng, T. (1999) Pharmacological activities of fusaric acid (5-butylpicolinic acid). *Life sciences* **65**(9): 849-856.

Wang, Y., Zhou, C., Huo, J., Ni, Y., Zhang, P., Lu, C., Jing, B., Xiao, F., Chen, W., Li, W. and Zhang, P. (2015) TRAF6 is required for the GM-CSF-induced JNK, p38 and Akt activation. *Molecular immunology* **65**(2): .224-229.

Yumnam, S., Park, H.S., Kim, M.K., Nagappan, A., Hong, G.E., Lee, H.J., Lee, W.S., Kim, E.H., Cho, J.H., Shin, S.C. and Kim, G.S. (2014) Hesperidin induces paraptosis like cell death in hepatoblatoma, HepG2 cells: Involvement of ERK1/2 MAPK. *PloS one* **9**(6): e101321.

Zarubin, T. and Jiahuai, H. (2005) Activation and signaling of the p38 MAP kinase pathway. *Cell research* **15**(1): 11-18.

Zarzycki, M. and Tuszyńska, L. (2013) Cell Lines as a Model for Immune Cells in Research and Didactics. *The International Union of Biological Sciences* **54**: 170-182.

Zhang, W. and Liu, H.T. (2002) MAPK signal pathways in the regulation of cell proliferation in mammalian cells. *Cell research* **12**(1): 9-18.

Zhang, Y., Wang, X., Yang, H., Liu, H., Lu, Y., Han, L. and Liu, G. (2013) Kinase AKT controls innate immune cell development and function. *Immunology* **140**(2): 143-152.

Zhou, F., Yang, Y. and Xing, D. (2011) Bcl-2 and Bcl-xL play important roles in the crosstalk between autophagy and apoptosis. *FEBS journal* **278**(3): 403-413.

Zitvogel, L., Kepp, O. and Kroemer, G. (2010) Decoding cell death signals in inflammation and immunity. *Cell* **140**(6): 798-804.

APPENDICES

APPENDIX 1

Raw data used to determine the IC_{50} of PBMC and Thp-1 cell viability following a 24 hour exposure to varying FA concentrations.

Table 1: Cell viability of PBMCs treated with FA for 24 hours.

FA concentration (µg/ml)	Log [FA] concentration	Average optical density (OD)	Cell viability (%)
0		0,340	100
30	1,477121255	0,274	80,41
35	1,544068044	0,252	74,05
40	1,602059991	0,250	73,36
50	1,698970004	0,262	76,89
10	2	0,210	61,80
200	2,301029996	0,221	64,94
300	2,477121255	0,218	63,96

Table 2: Cell viability of Thp-1 cells treated with FA for 24 hours.

FA concentration (µg/ml)	Log [FA] concentration	Average optical density (OD)	Cell viability (%)
0		2,492	100
30	1,477121255	2,1223	85,19
35	1,544068044	2,082	83,57
40	1,602059991	2,099	84,23
50	1,698970004	2,010	80,68
10	2	1,294	51,93
200	2,301029996	0,140	5,63
300	2,477121255	0,120	4,83

APPENDIX 2

Flow cytometric analysis of Annexin V-FITC and Propidium iodide staining in PBMCs and Thp-1 cells treated with FA for 24 hours.

A

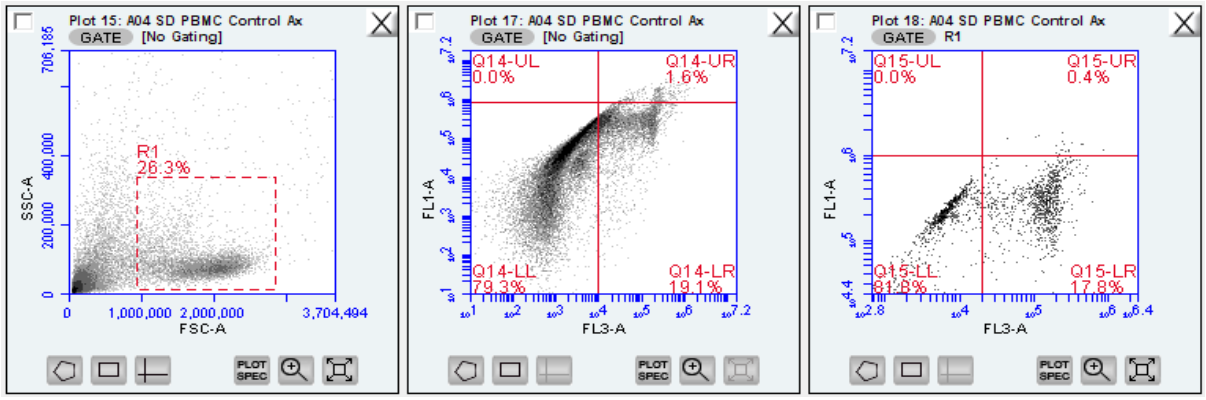

B

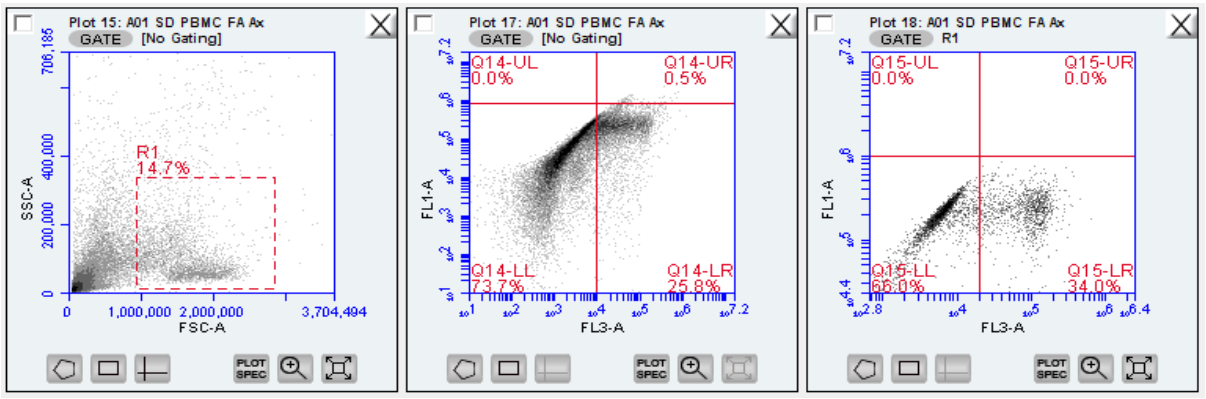

Figure 1: Dot plot with gate illustrating toxicity of FA in PBMC control (A) and FA treated (B) population stained with Annexin V-FITC and Propidium iodide.

A

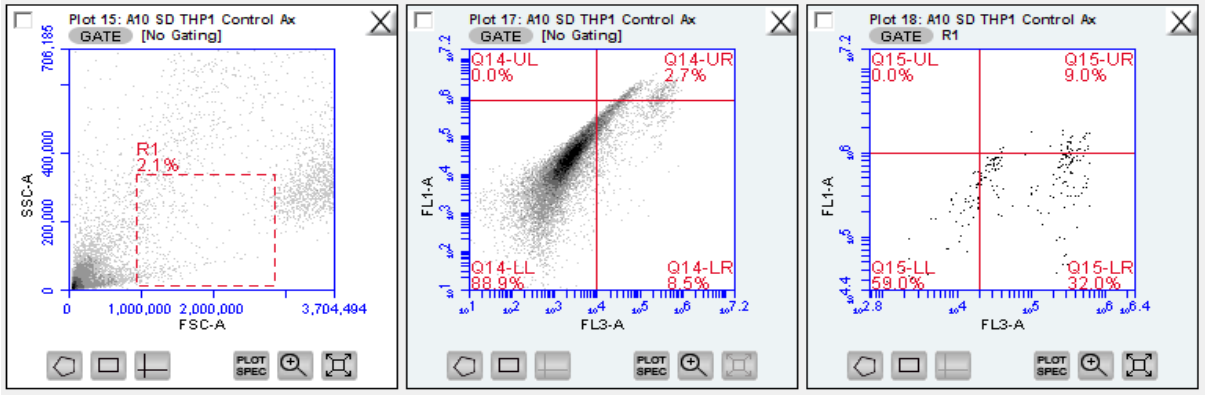

B

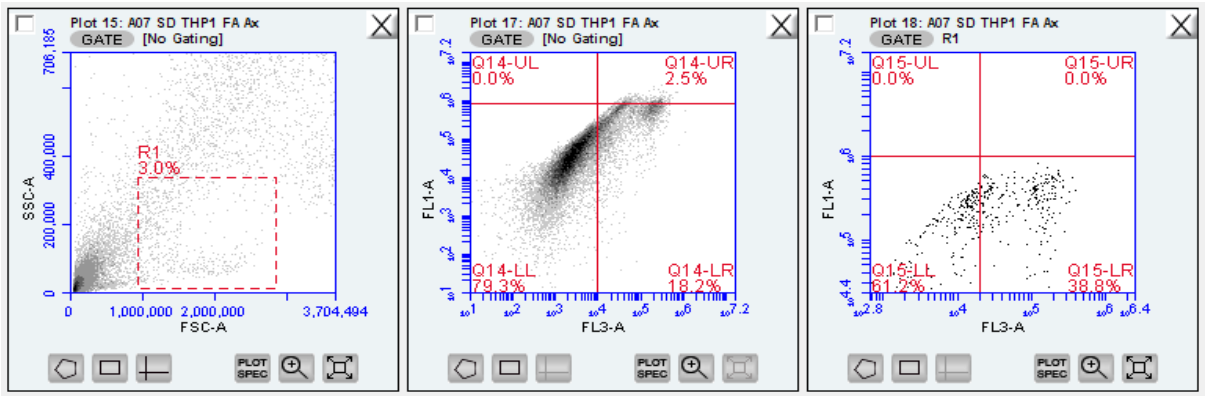

Figure 2: Dot plot with gate illustrating toxicity of FA in Thp-1 control (A) and FA treated (B) population with Annexin V-FITC and Propidium iodide.

A **B**

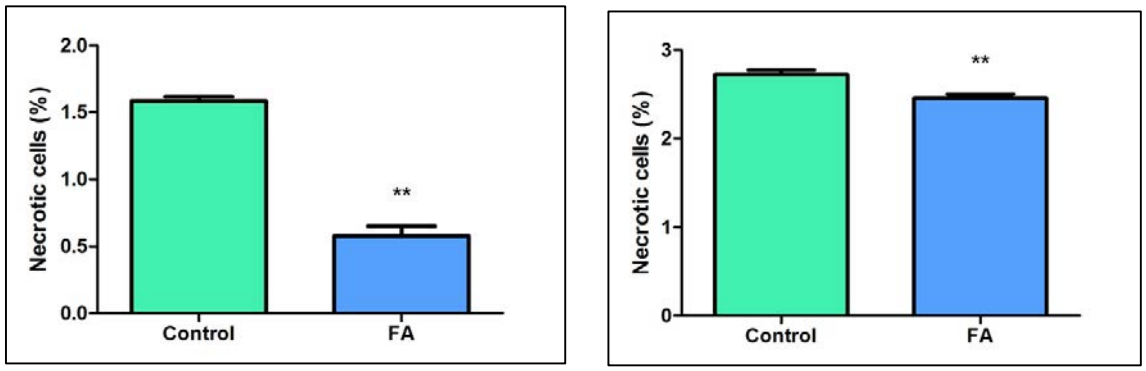

Figure 3: Effect of FA on necrotic cell death in PBMCs (A) and Thp-1 cells (B). **p<0.005.

APPENDIX 3

Detection of initiator (8, 9) and effector (3/7) caspase activities in PBMCs and Thp-1 cells treated with FA.

A **B**

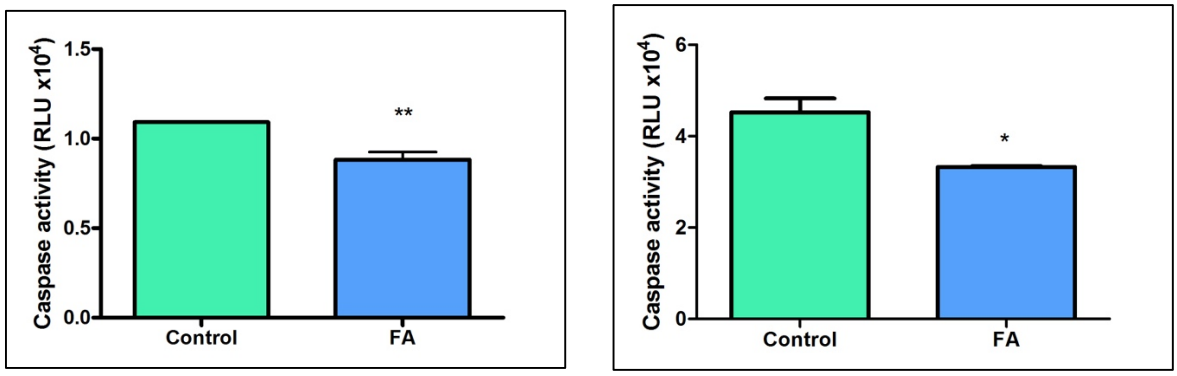

Figure 1: Caspase 8 activity in PBMCs (A) and Thp-1 cells (B) treated with FA. *p<0.05; **0.005.

A **B**

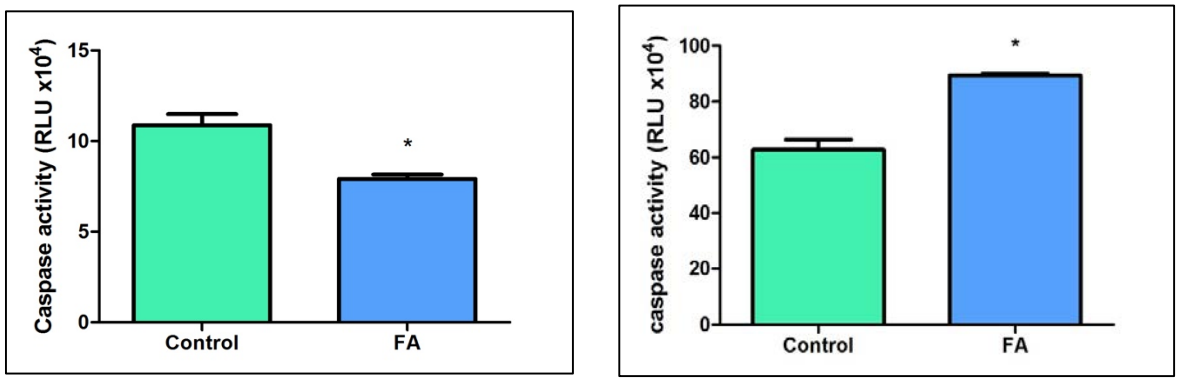

Figure 2: Caspase 9 activity in PBMCs (A) and Thp-1 cells (B) treated with FA. *p<0.05.

A **B**

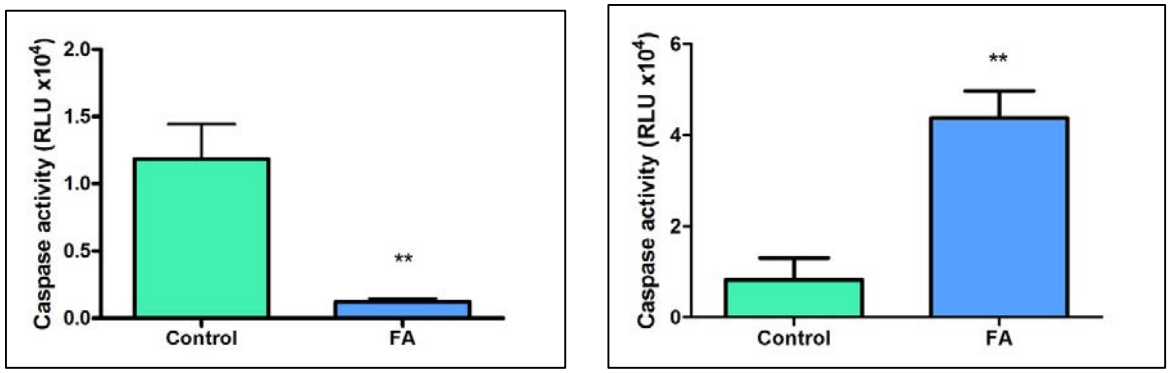

Figure 3: Caspase 3/7 activity in PBMCs (A) and Thp-1 cells (B) treated with FA. **p<0.005.

APPENDIX 4

Analysis of TNF-α cytokine levels in healthy PBMCs and Thp-1 cells treated with FA.

Table 1: Raw data used to construct the standard curve for TNF-α cytokine levels in PBMCs and Thp-1 cells exposed to FA for 24 hours.

Standards	Average OD (450nm)	Average OD – average negative control
0	0,093	-0,104583333
7,8	0,095	-0,102333333
15,6	0,099	-0,098083333
31,3	0,092	-0,105833333
62,5	0,120	-0,077083333
125	0,155	-0,042333333
250	0,237	0,039916667
500	0,396	0,198666667
Negative control	0,197	

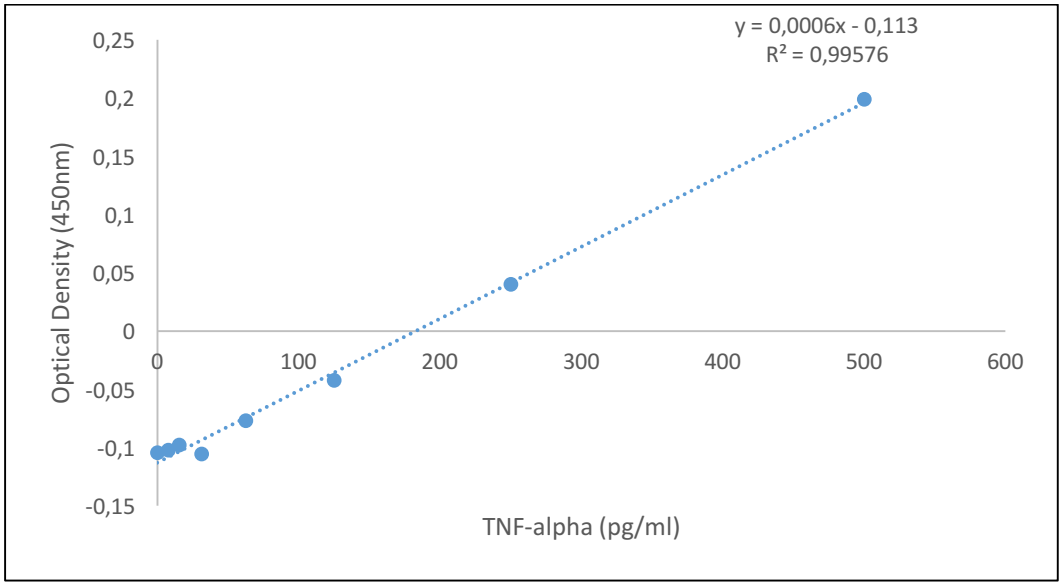

Figure 1: Standard curve used to determine TNF-α concentration levels in PBMCs and Thp-1 cells treated with FA using known TNF-α concentrations.

The equation $y = 0.006x - 0.113$ was used to calculate TNF-α concentrations in PBMC treated and untreated samples and Thp-1 treated and untreated samples.

APPENDIX 5

Calculation of MDA levels in PBMCs and Thp-1 cells

Table 1: MDA concentration levels in PBMCs and Thp-1 cells treated with FA for 24 hours.

Sample	Average OD	MDA concentration	
		(mM)	(µM)
PBMC C	0,006	0,000021	0,021
PBMC FA	0,028	0,000162	0,162
Thp-1 C	0,031	0,000179	0,179
T hp-1 FA	0,047	0,000284	0,284
Negative control	0,003		

APPENDIX 6

Flow cytometric analysis of JC-1 staining in PBMCs and Thp-1 cells treated with FA for 24 hours.

A

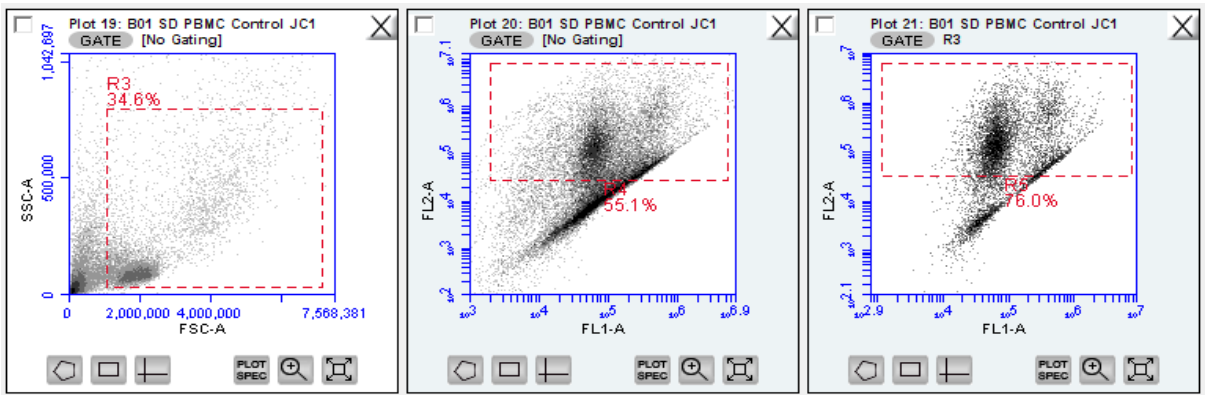

B

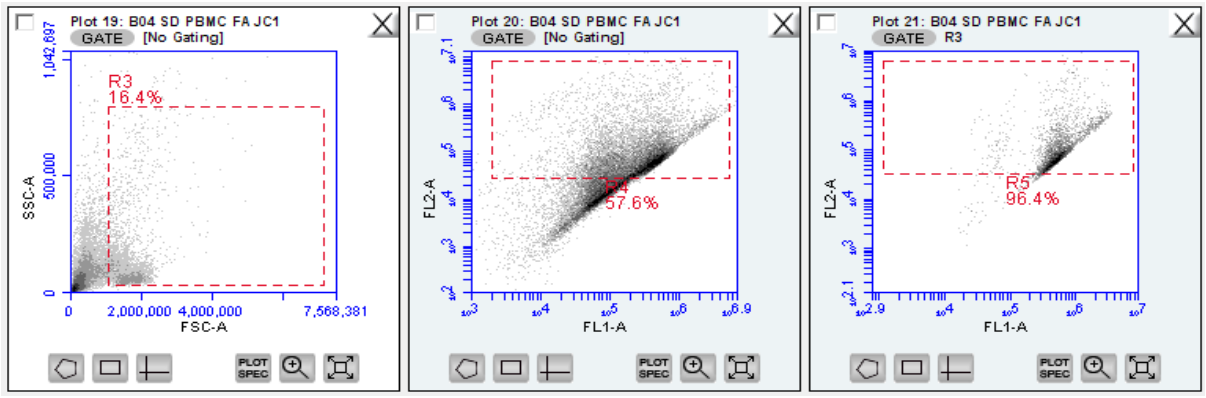

Figure 1: Dot plot with gate illustrating the effect of FA on mitochondrial membrane potential in PBMC control (A) and FA treated (B) cells stained with JC-1.

A

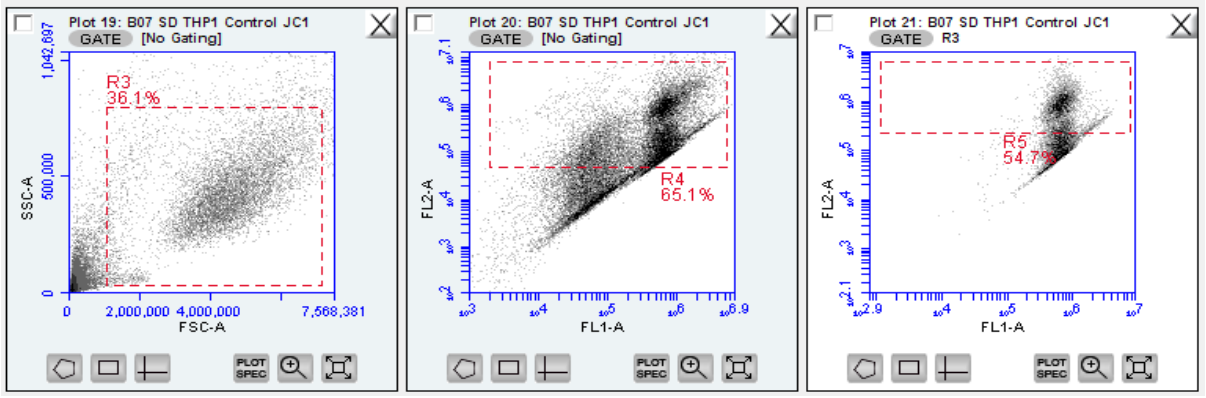

B

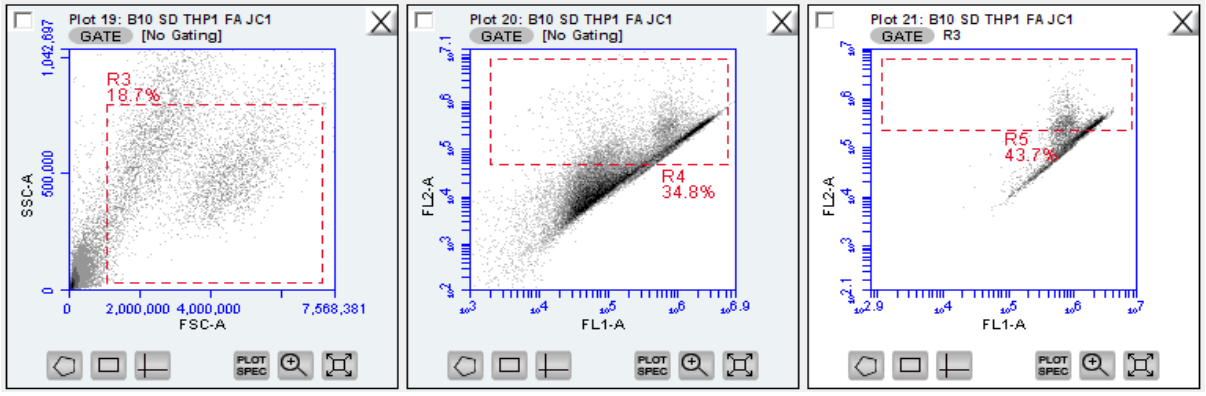

Figure 2: Dot plot with gate illustrating the effect of FA on mitochondrial membrane potential in PBMC control (A) and FA treated (B) cells stained with JC-1.

APPENDIX 7

Protein quantification and standardization of protein samples isolated from PBMC and Thp-1 cells treated with FA.

Table 1: Raw data used to construct the standard curve of BSA concentrations to determine protein quantity in PBMCs and Thp-1 cells exposed to FA for 24 hours.

Standards (mg/ml)	OD1	OD2	Average OD
0	0.165	0.131	0.148
0.2	0.315	0.371	0.343
0.4	0.614	0.542	0.578
0.6	0.835	0.704	0.770
0.8	0.949	0.867	0.908
1.0	1.196	1.194	1.195

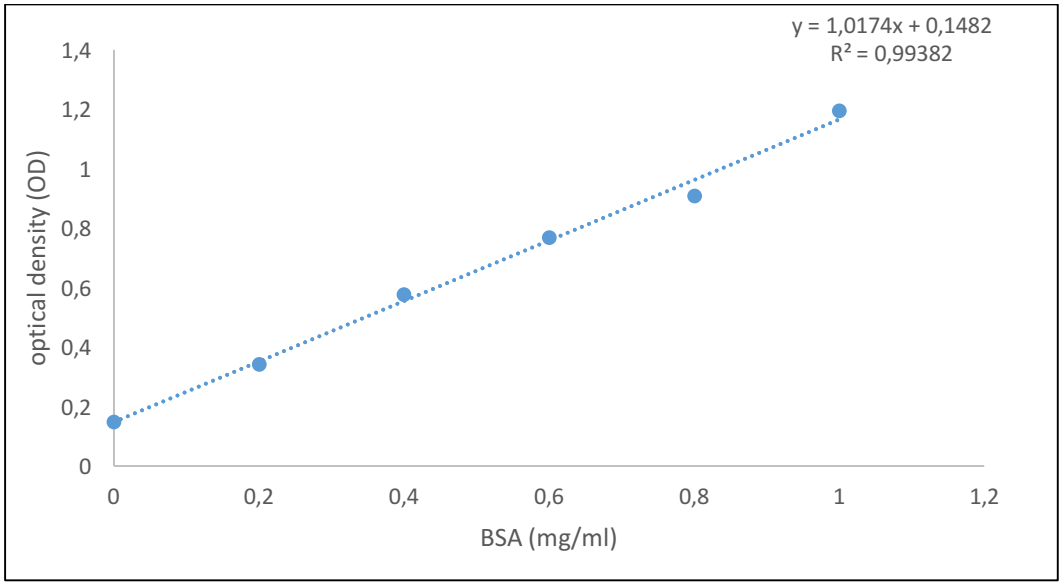

Figure 1: Standard curve used to determine the quantity of protein in PBMCs and Thp-1 cells treated with FA using known BSA concentrations.

The equation y = 1.0174x + 0.1482 was used to determine the concentration of protein in PBMC treated and untreated samples and Thp-1 treated and untreated samples.

Table 2: Protein quantification of PBMC and Thp-1 treated and untreated samples.

	OD1	OD2	Average OD	Concentration (mg/ml)
PBMC C	0.382	0.410	0.396	0.243
PBMC FA	0.558	0.508	0.533	0.378
Thp-1 C	1.936	1.968	1.952	1.773
Thp-1 FA	2.462	2.364	2.413	2.226

Table 3: Protein standardization of PBMC and Thp-1 samples.

Sample	Initial concentration (mg/ml)	Initial volume (µl)	Final concentration (mg/ml)	Final volume (µl)
PBMC C	0.243	98.765	0.200	120
PBMC FA	0.378	63.492	0.200	120
Thp-1 C	1.773	67.681	1.000	120
Thp-1 FA	2.226	53.908	1.000	120